A neurotrophin functioning with a Toll regulates structural plasticity in a dopaminergic circuit

Jun Sun[1], Francisca Rojo-Cortés[1], Suzana Ulian-Benitez[1,2], Manuel G. Forero[3], Guiyi Li[1], Deepanshu Singh[1], Xiaocui Wang[1], Sebastian Cachero[4], Marta Moreira[1], Dean Kavanagh[5], Gregory Jefferis[4], Vincent Croset[6], and Alicia Hidalgo[1*]

1, Structural Plasticity & Regeneration Group, School of Biosciences, University of Birmingham, UK;

2, Current address: Buck Institute for Research on Aging, California, US;

3, Semillero Lún, Grupo D+Tec, Universidad de Ibagué, Colombia;

4, MRC LMB, Cambridge, UK;

5, Institute of Biomedical Research, University of Birmingham, UK.

6, Department of Biosciences, Durham University, UK.

*Author for correspondence:

00 44 (0)121 4145416

a.hidalgo@bham.ac.uk

Keywords: Drosophila, structural plasticity, cell survival, synaptogenesis, neurodegeneration, DNT-2, Toll-6, Kek-6, Toll-Like Receptor, Kekkon, Kek.

ABSTRACT

Experience shapes the brain, as neural circuits can be modified by neural stimulation or the lack of it. The molecular mechanisms underlying structural circuit plasticity and how plasticity modifies behaviour, are poorly understood. Subjective experience requires dopamine, a neuromodulator that assigns a value to stimuli, and it also controls behaviour, including locomotion, learning and memory. In *Drosophila*, Toll receptors are ideally placed to translate experience into structural brain change. *Toll-6* is expressed in dopaminergic neurons (DANs), raising the intriguing possibility that Toll-6 could regulate structural plasticity in dopaminergic circuits. *Drosophila* neurotrophin-2 (DNT-2) is the ligand for Toll-6 and Kek-6, but whether it is required for circuit structural plasticity was unknown. Here, we show that *DNT-2* expressing neurons connect with DANs, and they modulate each other. Loss of function for *DNT-2* or its receptors *Toll-6* and kinase-less Trk-like *kek-6* caused DAN and synapse loss, impaired dendrite growth and connectivity, decreased synaptic sites and caused locomotion deficits. By contrast, over-expressed *DNT-2* increased DAN cell number, dendrite complexity and promoted synaptogenesis. Neuronal activity modified DNT-2, it increased synaptogenesis in DNT-2-positive neurons and DANs, and over-expression of DNT-2 did too. Altering the levels of DNT-2 or Toll-6 also modified dopamine-dependent behaviours, including locomotion and long-term memory. To conclude, a feedback loop involving dopamine and DNT-2 sculpted the circuits engaged, and DNT-2 with Toll-6 and Kek-6 induced structural plasticity in this circuit modifying brain function and behaviour.

53 **INTRODUCTION**

54 The brain can change throughout life, as new cells are formed or eliminated, axonal and dendritic arbours
55 can grow or shrink, synapses can form or be eliminated (Wiesel 1982, Feldman and Brecht 2005, Holtmaat
56 and Svoboda 2009, Gage 2019). Such changes can be driven by experience, that is, neuronal activity or the
57 lack of it (Wiesel 1982, Maguire et al. 2000, Cotman and Berchtold 2002, Feldman and Brecht 2005, Sur and
58 Rubenstein 2005, Holtmaat and Svoboda 2009, Woollett and Maguire 2011, Chen and Brumberg 2021,
59 Bharmauria et al. 2022). Structural changes result in remodelling of connectivity patterns, and these bring
60 about modifications of behaviour. These can be adaptive, dysfunctional or simply the consequence of
61 opportunistic connections between neurons (Kuner and Flor 2016, Leemhuis et al. 2019, Yang et al. 2020).
62 It is critical to understand how structural modifications to cells influence brain function. This requires
63 linking with cellular resolution molecular mechanisms, neural circuits and resulting behaviours.

64 In the mammalian brain, the neurotrophins (NTs: BDNF, NGF, NT3, NT4) are growth factors
65 underlying structural brain plasticity (Poo 2001, Lu et al. 2005, Park and Poo 2013). They promote neuronal
66 survival, connectivity, neurite growth, synaptogenesis, synaptic plasticity and Long-Term Potentiation (LTP),
67 via their Trk and $p75^{NTR}$ receptors (Poo 2001, Lu et al. 2005, Park and Poo 2013). In fact, all anti-depressants
68 function by stimulating production of BDNF and signalling via its receptor TrkB, leading to increased brain
69 plasticity (Casarotto et al. 2021, Castren and Monteggia 2021). Importantly, NTs have dual functions and
70 can also induce neuronal apoptosis, neurite loss, synapse retraction and Long-Term Depression (LTD), via
71 $p75^{NTR}$ and Sortilin (Lu et al. 2005). Remarkably, these latter functions are shared with neuroinflammation,
72 which in mammals involves Toll-Like Receptors (TLRs)(Squillace and Salvemini 2022). TLRs and Tolls have
73 universal functions in innate immunity across the animals (Gay and Gangloff 2007), and consistently with
74 this, TLRs in the CNS are mostly studied in microglia. However, mammalian *TLRs* are expressed in all CNS
75 cell types, where they can promote not only neuroinflammation, but also neurogenesis, neurite growth and
76 synaptogenesis and regulate memory – independently of pathogens, cellular damage or disease (Ma et al.
77 2006, Rolls et al. 2007, Okun et al. 2010, Okun et al. 2011, Patel et al. 2016, Chen, CY et al. 2019). Whether

78 TLRs have functions in structural brain plasticity and behaviour remains little explored, and whether they
79 can function together with neurotrophins in the mammalian brain is unknown.

80 Progress linking cellular and molecular events to circuit and behavioural modification has been
81 rather daunting and limited using mammals (Wang et al. 2022). The *Drosophila* adult brain is plastic and
82 can be modified by experience and neuronal activity (Technau 1984, Barth and Heisenberg 1997, Barth et
83 al. 1997, Sachse et al. 2007, Kremer et al. 2010, Sugie et al. 2015, Linneweber et al. 2020, Baltruschat et al.
84 2021, Coban et al. 2024). Different living conditions, stimulation with odorants or light, circadian rhythms,
85 nutrition, long-term memory and experimentally activating or silencing neurons, modify brain volume, alter
86 circuit and neuronal shape, and remodel synapses, revealing experience-dependent structural plasticity
87 (Heisenberg et al. 1995, Barth and Heisenberg 1997, Barth et al. 1997, Devaud et al. 2001, Gorska-
88 Andrzejak et al. 2005, Sachse et al. 2007, Fernandez et al. 2008, Kremer et al. 2010, Bushey et al. 2011,
89 Sugie et al. 2015, Duhart et al. 2020, Baltruschat et al. 2021, Vaughen et al. 2022, Coban et al. 2024).
90 Furthermore, the *Drosophila* brain is also susceptible to neurodegeneration (Bolus et al. 2020). However,
91 the molecular and circuit mechanisms underlying structural brain plasticity are mostly unknown in
92 *Drosophila*.

93 *Toll* receptors are expressed across the *Drosophila* brain, in distinct but overlapping patterns that
94 mark the anatomical brain domains (Li et al. 2020). Tolls share a common signalling pathway downstream,
95 that can drive at least four distinct cellular outcomes – cell death, survival, quiescence, proliferation –
96 depending on context (McIlroy et al. 2013, Foldi et al. 2017, Anthoney et al. 2018, Li et al. 2020). They are
97 also required for connectivity and structural synaptic plasticity and they can also induce cellular events
98 independently of signalling (McIlroy et al. 2013, Ward et al. 2015, McLaughlin et al. 2016, Foldi et al. 2017,
99 Ulian-Benitez et al. 2017, Li et al. 2020). These nervous system functions occur in the absence of tissue
100 damage or infection. This is consistent with the fact that - as well as universal functions in innate immunity
101 - Tolls also have multiple non-immune functions also outside the CNS, including the original discovery of
102 Toll in dorso-ventral patterning, cell intercalation, cell competition and others (Meyer et al. 2014, Pare et
103 al. 2014, Anthoney et al. 2018, Tamada et al. 2021). The Toll distribution patterns in the adult brain and

104 their ability to switch between distinct cellular outcomes means they are ideally placed to translate
105 experience into structural brain change (Li et al. 2020).
106 We had previously observed that in the adult brain, *Toll-6* is expressed in dopaminergic neurons
107 (McIlroy et al. 2013). Dopamine is a key neuromodulator that regulates wakefulness and motivation,
108 experience valence, such as reward, and it is essential for locomotion, learning and memory
109 (Riemensperger et al. 2011, Waddell 2013, Adel and Griffith 2021). In *Drosophila*, Dopaminergic neurons
110 (DANs) form an associative neural circuit together with mushroom body Kenyon cells (KCs), Dorsal Anterior
111 Lateral neurons (DAL) and Mushroom Body Output neurons (MBONs) (Chen et al. 2012, Aso et al. 2014a,
112 Boto et al. 2020, Adel and Griffith 2021). Kenyon cells receive input from projection neurons of the sensory
113 systems, they then project through the mushroom body lobes where they are intersected by DANs to
114 regulate MBONs to drive behaviour (Heisenberg 2003, Aso et al. 2014b, Boto et al. 2020). This associative
115 circuit is required for learning, long-term memory and goal-oriented behaviour (Chen et al. 2012, Guven-
116 Ozkan and Davis 2014, Adel and Griffith 2021). During experience, involving sensory stimulation from the
117 external world and from own actions, dopamine assigns a value to otherwise neutral stimuli, labelling the
118 neural circuits engaged (Boto et al. 2020). Thus, this raises the possibility that a link of Toll-6 to dopamine
119 could enable translating experience into circuit modification to modulate behaviour.
120 In *Drosophila*, Toll receptors can function both independently of ligand-binding and by binding
121 Spätzle (Spz) protein family ligands, also known as *Drosophila* neurotrophins (DNTs), that are sequence,
122 structural and functional homologues of the mammalian NTs (DeLotto and DeLotto 1998, Weber et al.
123 2003, Hoffmann et al. 2008a, Hoffmann et al. 2008b, Zhu et al. 2008, Lewis et al. 2013, McIlroy et al. 2013,
124 Foldi et al. 2017). Like mammalian NTs, DNTs also promote cell survival, connectivity, synaptogenesis and
125 structural synaptic plasticity, and they can also promote cell death, depending on context (Zhu et al. 2008,
126 McIlroy et al. 2013, Sutcliffe et al. 2013, Foldi et al. 2017, Ulian-Benitez et al. 2017). As well as Tolls, DNTs
127 are also ligands for Kekkon (Kek) receptors, kinase-less homologues of the mammalian NT Trk receptors
128 and are required for structural synaptic plasticity (Ulian-Benitez et al. 2017). Importantly, the targets
129 regulated by Tolls and Keks - ERK, NFκB, PI3K, JNK, CaMKII – are shared with those of mammalian NT

130 receptors Trk and p75^{NTR}, and have key roles in structural and functional plasticity across the animals (Park
131 and Poo 2013, Foldi et al. 2017, Ulian-Benitez et al. 2017, Yang et al. 2020, Tamada et al. 2021).
132 Here, we focus on Drosophila neurotrophin -2 (DNT-2), proved to be the ligand of Toll-6 and Kek-6,
133 with in vitro, cell culture and in vivo evidence (McIlroy et al. 2013, Foldi et al. 2017, Ulian-Benitez et al.
134 2017). Here we asked how DNT-2, Toll-6 and Kek-6 are functionally related to dopamine, whether they and
135 neuronal activity – as a proxy for experience - can modify neural circuits, and how structural circuit
136 plasticity modifies dopamine-dependent behaviours.
137
138 RESULTS
139 **DNT-2A, Toll-6 and Kek-6 neurons are integrated in a dopaminergic circuit**
140 To allow morphological and functional analyses of *DNT-2* expressing neurons, we generated a *DNT-2Gal4*
141 line using CRISPR/Cas9 and drove expression of the membrane-tethered-GFP *FlyBow1.1* reporter. We
142 identified at least 12 DNT-2+ neurons and we focused on four anterior DNT-2A neurons per hemi-brain
143 (Figure 1A, B). Using the post-synaptic marker Denmark, DNT-2A dendrites were found at the prow (PRW)
144 and flange (FLA) region, whereas axonal terminals visualised with the pre-synaptic marker synapse
145 defective 1 (Dsyd1-GFP) resided at the superior medial protocerebrum (SMP) (Figure 1C, C''). We
146 additionally found post-synaptic signal at the SMP and pre-synaptic signal at the FLA/PRW (Figure 1C, C'),
147 suggesting bidirectional communication at both sites. Using Multi-Colour Flip-Out (MCFO) to label
148 individual cells stochastically (Nern et al. 2015, Costa et al. 2016), single neuron clones revealed variability
149 in the DNT-2A projections across individual flies (Figure 1D), consistently with developmental and activity-
150 dependent structural plasticity in *Drosophila* (Heisenberg et al. 1995, Kremer et al. 2010, Sugie et al. 2015,
151 Mayseless et al. 2018, Li et al. 2020, Linneweber et al. 2020, Baltruschat et al. 2021). We found that DNT-2A
152 neurons are glutamatergic as they express the vesicular glutamate transporter vGlut (Figure 1E, Figure S1A)
153 and lack markers for other neurotransmitter types (Figure S1). DNT-2A terminals overlapped with those of
154 dopaminergic neurons (Figure 1G), suggesting they could receive inputs from neuromodulatory neurons. In
155 fact, single-cell RNA-seq revealed transcripts encoding the dopamine receptors *Dop1R1, Dop1R2, Dop2R*

156 and/or *DopEcR* in DNT-2+ neurons (Croset et al. 2018). Using reporters, we found that Dop2R is present in
157 DNT-2A neurons (Figure 1F, Figure S1B), but not Dop1R2 (Figure S1E). Altogether, these data showed that
158 DNT-2A neurons are glutamatergic neurons that could receive dopaminergic input both at PRW and SMP.
159 DNT-2 functions via Toll-6 and Kek-6 receptors, and *Toll-6* is expressed in DANs (McIlroy et al. 2013).
160 To identify the cells expressing *Toll-6* and *kek-6* and explore further their link to the dopaminergic system,
161 we used *Toll-6Gal4 (Li et al. 2020)* and *kek-6Gal4* (Ulian-Benitez et al. 2017) to drive expression of
162 membrane-tethered *FlyBbow1.1* and assessed their expression throughout the brain. Using anti-Tyrosine
163 Hydroxilase (TH) - the enzyme that catalyses the penultimate step in dopamine synthesis - to visualise
164 DANs, we found that Toll-6+ neurons included dopaminergic neurons from the PAMs, PPL1 and PPL2
165 clusters (Figure 1I, Figure S2D,F Table S1), whilst Kek-6+ neurons included PAM, PAL, PPL1, PPM2 and PPM3
166 dopaminergic clusters (Figure 1J, Figure S2B,E,F Table S1). DNT-2 can also bind various Tolls and Keks
167 promiscuously (McIlroy et al. 2013, Foldi et al. 2017) and other *Tolls* are also expressed in the dopaminergic
168 system: PAMs express multiple *Toll* receptors (Figure S2F) and all PPL1s express at least one *Toll* (Figure
169 S2F). Using MCFO clones revealed that both *Toll-6* and *kek-6* are also expressed in Kenyon cells (Li et al.
170 2020) (Figure S2I,J, Table S1), DAL neurons (Figure S2G,H, Table S1) and MBONs (Figure S2A-C). In summary,
171 *Toll-6* and *kek-6* are expressed in DANs, DAL, Kenyon cells and MBONs (Figure 1H). These cells belong to a
172 circuit required for associative learning, long-term memory and behavioural output, and DANs are also
173 required for locomotion (Riemensperger et al. 2011, Chen et al. 2012, Aso et al. 2014b, Boto et al. 2014,
174 Adel and Griffith 2021, Huang et al. 2024). Altogether, our data showed that DNT-2A neurons are
175 glutamatergic neurons that could receive dopamine as they contacted DANs and expressed the *Dop2R*
176 receptor, and that in turn DANs expressed the DNT-2 receptors *Toll-6* and *kek-6*, and therefore could
177 respond to DNT-2. These data suggested that there could be bidirectional connectivity between DNT-2A
178 neurons and DANs, which we explored below.
179
180 **Bidirectional connectivity between DNT-2A neurons and DANs**

181 To verify the connectivity of DNT-2A neurons with DANs, we used various genetic tools. To identify DNT-2A
182 output neurons, we used TransTango (Talay et al. 2017) (Figure 2A and Figure S3). DNT-2A RFP+ outputs
183 included a subset of MB α'β' lobes, αβ Kenyon cells, tip of MB β'2, DAL neurons, dorsal fan-shaped body
184 layer and possibly PAM or other dopaminergic neurons (Figure 2A, Figure S3). Consistently, these DNT-2A
185 output neurons express *Toll-6* and *kek-6* (Supplementary Table S1). To identify DNT-2A input neurons, we
186 used BAcTrace (Cachero et al. 2020). This identified PAM-DAN inputs at SMP (Figure 2B). Altogether, these
187 data showed that DNT-2A neurons receive dopaminergic neuromodulatory inputs, their outputs include
188 MB Kenyon cells, DAL neurons and possibly DANs, and DNT-2 arborisations at SMP are bidirectional.
189 To further test the relationship between DNT-2A neurons and DANs, we reasoned that stimulating
190 DANs would provoke either release or production of dopamine. So, we asked whether increasing DNT-2
191 levels in DNT-2 neurons could influence dopamine levels. For this, we over-express *DNT-2* in full-length
192 form (i.e. *DNT-2FL*), as it enables to investigate non-autonomous functions of DNT-2 (Ulian-Benitez et al.
193 2017). Importantly, DNT-2FL is spontaneously cleaved into the mature form (McIlroy et al. 2013, Foldi et al.
194 2017) (see discussion). Thus, we over-expressed *DNT-2FL* in DNT-2 neurons and asked whether this
195 affected dopamine production, using mRNA levels for *TH* as readout. Using quantitative real-time PCR (qRT-
196 PCR) we found that over-expressing *DNT2-FL* in DNT-2 neurons in adult flies increased *TH* mRNA levels in fly
197 heads (Figure 2C). This showed that DNT-2 could stimulate dopamine production.
198 Next, we wondered whether in turn DNT-2A neurons, that express *Dop2R*, could be modulated by
199 dopamine. Binding of dopamine to D2-like Dop2R (also known as DD2R) inhibits adenylyl-cyclase,
200 decreasing cAMP levels (Hearn et al. 2002, Neve et al. 2004). Thus, we asked whether DNT-2A neurons
201 received dopamine and signal via Dop2R. Genetic restrictions did not allow us to activate PAMs and test
202 DNT-2 neurons, so we activated DNT-2 neurons and tested whether *Dop2R* knock-down would increase
203 cAMP levels. We used the FRET-based cAMP sensor, Epac1-camps-50A (Shafer et al. 2008). When Epac1-
204 camps-50A binds cAMP, FRET is lost, resulting in decreased YFP/CFP ratio over time. Indeed, *Dop2R* RNAi
205 knock-down in DNT-2A neurons significantly increased cAMP levels (Figure 2D), demonstrating that
206 normally Dop2R inhibits cAMP signalling in DNT-2A cells. Importantly, this result meant that in controls,

207 activating DNT-2A neurons caused dopamine release from DANs that then bound Dop2R to inhibit adenylyl-
208 cyclase in DNT-2A neurons; this inhibition was prevented with *Dop2R* RNAi knock-down. Altogether, this
209 shows that DNT-2 up-regulated TH levels (Figure 2E), and presumably via dopamine release, this inhibited
210 cAMP in DNT-2A neurons (Figure 2F).

211 In summary, DNT-2A neurons are connected to DANs, DAL and MB Kenyon cells, all of which
212 express DNT-2 receptors *Toll-6* and *kek-6* and belong to a dopaminergic as well as associative learning and
213 memory circuit. Furthermore, DNT-2A and PAM neurons form bidirectional connectivity. Finally, DNT-2 and
214 dopamine regulate each other: DNT-2 increased dopamine levels (Figure 2E), and in turn dopamine via
215 Dop2R inhibited cAMP signalling in DNT-2A neurons (Figure 2F). That is, an amplification was followed by
216 negative feedback. This suggested that a dysregulation in this feedback loop could have consequences for
217 dopamine-dependent behaviours and for circuit remodelling by the DNT-2 growth factor.
218

219 **DNT-2 and Toll-6 maintain survival of PAM dopaminergic neurons in the adult brain**

220 Above we showed that DNT-2 and PAM dopaminergic neurons are connected, so we next asked whether
221 loss of function for *DNT-2* or *Toll-6* would affect PAMs. In wild-type flies, PAM-DAN number can vary
222 between 220-250 cells per *Drosophila* brain, making them ideal to investigate changes in cell number (Liu
223 et al. 2012). Maintenance of neuronal survival is a manifestation of structural brain plasticity in mammals,
224 where it depends on the activity-dependent release of the neurotrophin BDNF (Lu et al. 2005, Wang et al.
225 2022). Importantly, cell number can also change in the adult fly, as neuronal activity can induce
226 neurogenesis via Toll-2, whereas DANs are lost in neurodegeneration models (Feany and Bender 2000, Li et
227 al. 2020). Thus, we asked whether DNT-2 influences PAM-DAN number in the adult brain. We used *THGal4;*
228 *R58E02Gal4* to visualise nuclear Histone-YFP in DANs (Figure 3A) and counted automatically YFP+ PAMs
229 using a purposely modified DeadEasy plug-in developed for the adult fly brain (Li et al 2020). DeadEasy
230 plug-ins were developed and used before to count cells labelled with sparsely distributed nuclear markers
231 in embryos (Zhu et al. 2008, Forero et al. 2009, Forero et al. 2010a, Forero et al. 2010b, McIlroy et al. 2013),
232 larvae (Kato et al. 2011, Forero et al. 2012, Losada-Perez et al. 2016) and adult (Li et al. 2020) *Drosophila*

233 brains. Here we show that *DNT2*^{37}/*DNT2*^{18} mutant adult brains had fewer PAMs than controls (Figure 3B).
234 Similarly, *Toll-6* RNAi knock-down in DANs also decreased PAM neuron number (Figure 3C). DAN loss was
235 confirmed with anti-TH antibodies and counted manually, as there were fewer TH+ PAMs in *DNT2*^{37}/*DNT2*^{18}
236 mutants (Figure 3D). Importantly, PAM cell loss was rescued by over-expressing activated *Toll-6*^{CY} in DANs
237 in *DNT-2* mutants (Figure 3D). Altogether, these data showed that DNT-2 functions via Toll-6 to maintain
238 PAM neuron survival.

239 To ask whether DNT-2 could regulate dopaminergic neuron number specifically in the adult brain,
240 we used *tubGal80*^{ts} to conditionally knock-down gene expression in the adult. PAMs were visualised with
241 either *R58E02LexA>LexAop-nls-tdTomato* or *THGal4; R58E02Gal4 >histone-YFP* and counted automatically.
242 Adult specific *DNT-2* RNAi knock-down decreased Tomato+ PAM cell number (Figure 3E). Similarly, RNAi
243 *Toll-6* knock-down in DANs also decreased PAM neuron number (Figure 3F). Furthermore, knock-down of
244 either *Toll-6* or *DNT-2* in the adult brain caused loss of PAM neurons visualised with anti-TH antibodies and
245 counted manually (Figure 3G). Cell loss was due to cell death, as adult specific *DNT-2 RNAi* knock-down
246 increased the number of apoptotic cells labelled with anti-*Drosophila* Cleave caspase-1 (DCP-1) antibodies
247 compared to controls, including Dcp-1+ PAMs and other TH+ cells (Figure 3H). Dcp-1+ cells also included
248 TH-negative cells, consistent with the expression of *Toll-6* and *kek-6* also in other cell types. By contrast,
249 *DNT-2FL* over-expression in DNT2 neurons did not alter the incidence of apoptosis (Figure 3G), consistently
250 with the fact that DNT-2FL spontaneously cleaves into the mature form (McIlroy et al. 2013, Foldi et al.
251 2017). Instead, and importantly, over-expression of DNT-2FL increased PAM cell number (Figure 3G). Thus,
252 *DNT-2* and *Toll-6* knock-down specifically in the adult brain induced apoptosis and PAM-neuron loss,
253 whereas DNT-2 gain of function increased PAM cell number.

254 Altogether, these data showed that PAM cell number is plastic, sustained PAM neuron survival in
255 development and in the adult brain depends on DNT-2 and Toll-6, and a reduction in their levels causes
256 DAN cell loss, characteristic of neurodegeneration.

257

258 **DNT-2 and its receptors are required for arborisations and synapse formation**

259 We next asked whether DNT-2, Toll-6 and Kek-6 could influence dendritic and axonal arbours and synapses
260 of dopaminergic neurons (Figure 4A). Visualising the pre-synaptic reporter Synaptotagmin-GFP (Syt-GFP) in
261 all DANs, we found that *DNT-2*^{18}*/DNT-2*^{37} mutants completely lacked DAN synapses in the MB β,β' and
262 γ lobes (Figure 4B). Interestingly, DAN connections at α,α' lobes were not affected (Figure 4B). This means
263 that DNT-2 is required for synaptogenesis and connectivity of PAMs to MB β,β' and γ lobes.

264 PAM-β2β'2 neuron dendrites overlap axonal DNT2 projections. *Toll-6* RNAi knock-down in PAM -
265 β2β'2 (with split-GAL4 *MB301BGal4* (Aso et al. 2014a)), reduced dendrite complexity (Figure 4C). To test
266 whether DNT-2 could alter these dendrites, we over-expressed mature *DNT-2CK*. DNT-2CK is not secreted
267 (from transfected S2 cells), but it is functional in vivo (Zhu et al. 2008, Foldi et al. 2017, Ulian-Benitez et al.
268 2017). Importantly, over-expressed *DNT-2CK* functions cell-autonomously whereas *DNT-2FL* functions also
269 non-autonomously, but they have similar effects (Zhu et al. 2008, Foldi et al. 2017, Ulian-Benitez et al.
270 2017). Over-expression of *DNT-2CK* in PAM-β2β'2 increased dendrite arbour complexity (Figure 4D). Thus,
271 DNT-2 and its receptor Toll-6 are required for dendrite growth and complexity in PAM neurons.

272 To ask whether DNT-2 could affect axonal terminals, we tested PPL1 axons. PPL1-γ1-pedc neurons
273 have a key function in long-term memory gating (Aso et al. 2012, Placais et al. 2012, Aso et al. 2014a, Boto
274 et al. 2020, Huang et al. 2024) and express both *Toll-6* and *kek-6* (Table S1). Using split-GAL4 line M*B320C-*
275 *Gal4* to visualise PPL1 axonal arbours, RNAi knock-down of either *Toll-6*, *kek-6* or both together caused
276 axonal misrouting away from the mushroom body peduncle (Figure 4E,E', Chi Square $p<0.05$, see Table S2).
277 Similarly, *DNT-2FL* over-expression also caused PPL1 misrouting (Figure 4F, Chi-Square $p<0.05$, see Table
278 S2). Thus, DNT-2, Toll-6 and Kek-6 are required for appropriate targeting and connectivity of PPL1 DAN
279 axons.

280 To test whether this signalling system was required specifically in the adult brain, we used *tubGAL80*^{ts}
281 to knock-down *Toll-6* and *kek-6* with RNAi conditionally in the adult and visualised the effect on
282 synaptogenesis using the post-synaptic reporter Homer-GCaMP and anti-GFP antibodies. Adult-specific
283 *Toll-6 kek-6* RNAi knock-down in PAM neurons did not affect synapse number (not shown), but it decreased
284 post-synaptic density size, both at the MB lobe and at the SMP dendrite (Figure 4G). These data meant that

285 the DNT-2 receptors *Toll-6* and *kek-6* continue to be required in the adult brain for appropriate
286 synaptogenesis.
287 Altogether, these data showed that DNT-2, Toll-6 and Kek-6 are required for dendrite branching,
288 axonal targeting and synapse formation. The shared phenotypes from altering the levels of *DNT-2* and *Toll-*
289 *6 kek-6* in arborisations and synapse formation, support their joint function in these contexts. Importantly,
290 these findings showed that connectivity of PAM and PPL1 dopaminergic neurons depend on DNT-2, Toll-6
291 and Kek-6.
292
293 **DNT-2 neuron activation and *DNT-2* over-expression induced synapse formation in target PAM**
294 **dopaminergic neurons**
295 The above data showed that DNT-2, Toll-6 and Kek-6 are required for DAN cell survival, arborisations and
296 synaptogenesis in development and adults. This meant that the dopaminergic circuit remains plastic in
297 adult flies, consistently with their functional plasticity (Boto et al. 2014). Thus, we wondered whether
298 neuronal activity could also induce remodelling in PAM neurons. In mammals, neuronal activity induces
299 translation, release and cleavage of BDNF, and BDNF drives synaptogenesis (Poo 2001, Lu et al. 2005, Lu et
300 al. 2013, Wang et al. 2022). Thus, we first asked whether neuronal activity could influence DNT-2 levels or
301 function. We visualised tagged DNT-2FL-GFP in adult brains, activated DNT-2 neurons with TrpA1 at 30°C,
302 and found that DNT-2 neuron activation increased the number of DNT-2-GFP vesicles produced
303 (Supplementary Figure S4A). Furthermore, neuronal activity also facilitated cleavage of DNT-2 into its
304 mature form. In western blots from brains over-expressing *DNT-2FL-GFP*, the levels of full-length DNT-2FL-
305 GFP were reduced following neuronal activation and the cleaved DNT-2CK-GFP form was most abundant
306 (Supplementary Figure S4B). These findings meant that, like mammalian BDNF, also DNT-2 can be
307 influenced by activity.
308 Thus, we asked whether neuronal activity and DNT-2 could influence synapse formation. We first
309 tested DNT-2 neurons. Activating DNT-2 neurons altered DNT-2 axonal arbours (Figure 5A) and it increased
310 Homer-GFP+ synapse number in the DNT-2 SMP arbour (Figure 5B and Figure S5). Next, as DNT-2 and PAMs

311 form bidirectional connexions at SMP (Figure 1, 2), we asked whether activating DNT-2 neurons could
312 affect target PAM neurons. To manipulate DNT-2 neurons and visualise PAM neurons concomitantly, we
313 combined *DNT-2GAL4* with the *PAM-LexAOP* driver. However, there were no available *LexA/OP* post-
314 synaptic reporters, so we used the pre-synaptic *LexAOP-Syt-GCaM*P reporter instead, which labels
315 Synaptotagmin (Syt), and GFP antibodies. Activating DNT-2 neurons with TrpA1 increased the number of
316 Syt+ synapses at the PAM SMP arbour (Figure 5C) and reduced their size (Figure 5C). This was consistent
317 with the increase in Homer-GFP+ PSD number in stimulated DNT-2 neurons (Figure 5B). Neuronal activity
318 can induce ghost boutons, immature synapses that are later eliminated (Fuentes-Medel et al. 2009). Here,
319 the coincidence of increased pre-synaptic Syt-GFP from PAMs and post-synaptic Homer-GFP from DNT-2
320 neurons at SMP suggests that newly formed synapses could be stable. PAM neurons also send an
321 arborisation at the MB β, β', γ lobes, but DNT-2 neuron activation did not affect synapse number nor size
322 there (Figure 5C). These data showed that activating DNT-2 neurons induced synapse formation at the SMP
323 connection with PAMs.
324 Finally, we asked whether, like activity, DNT-2FL could also drive synaptogenesis. We over-expressed
325 *DNT-2FL* in DNT-2 neurons and visualised the effect in PAM neurons. Over-expression of *DNT-2FL* in DNT-2
326 neurons did not alter Syt+ synapse number at the PAM SMP dendrite, but it increased bouton size (Figure
327 5D). By contrast, at the MB β, β' lobe arborisation, over-expressed *DNT-2* did not affect Syt+ bouton size,
328 but it increased the number of output synapses (Figure 5D). This data showed that DNT-2 released from
329 DNT-2 neurons could induce synapse formation in PAM target neurons.
330 Altogether, these data showed that neuronal activity induced synapse formation, it stimulated
331 production and cleavage of DNT-2, and DNT-2 could induce synapse formation in target neurons.
332
333 **Structural plasticity by DNT2 modified dopamine-dependent behaviour**
334 Circuit structural plasticity raises the important question of what effect it could have on brain function, i.e.
335 behaviour. Data above showed that DANs and DNT-2 neurons are functionally connected, that loss of
336 function for *DNT-2* or its receptors caused dopaminergic neuron loss, altered DAN arborisations and caused

337 synapse loss or reduction in size, and that DNT-2 could induce dendrite branching and synaptogenesis,
338 altogether modifying circuit connectivity. To measure the effect of such circuit modifications on brain
339 function, we used dopamine-dependent behaviours as readout.

340 Startle-induced negative geotaxis (also known as the climbing assay) is commonly used as a
341 measure of locomotor ability and requires dopamine and specifically PAM neuron function (Riemensperger
342 et al. 2013, Sun et al. 2018). We tested the effect of *DNT-2* or *Toll-6* and *kek-6* loss of function in climbing,
343 and both *DNT-2*^{37}/*DNT-2*^{18} mutants and flies in which *DNT-2* was knocked-down in DNT-2 neurons in the
344 adult stage had lower climbing ability than controls (Figure 6A). Similarly, when *Toll-6* and *kek-6* were
345 knocked-down with RNAi in the adult using a *Toll-6*- or a *PAM-GAL4* neuron driver, climbing was also
346 reduced (Figure 6B). Importantly, over-expressing activated *Toll-6*^{CY} in DANs rescued the locomotion
347 deficits of *DNT-2* mutants, showing that DNT-2 functions via Toll-6 in this context (Figure 6C).

348 We also tracked freely moving flies in an open arena (Eyjolfsdottir et al. 2014). Interestingly, in that
349 setting, locomotion of homozygous *DNT-2*^{37}/*DNT-2*^{18} mutants was similar to that of controls, but over-
350 expression of *Toll-6*^{CY} in their DANs increased locomotion as flies walked longer distances and spent less
351 time immobile (Figure 6D). Adult flies over-expressing *DNT2-FL* walked faster (Figure 6E and Figure S5) and
352 so did those where DNT-2 neurons were activated with TrpA1 (Figure 6F and Figure S6), consistently with
353 the fact that neuronal activity increased DNT-2 production (Figure S4A) and that DNT-2FL increased TH
354 levels (Figure 2C). Therefore, increased Toll-6^{CY} levels in DANs increase locomotion and increased DNT-2
355 levels are sufficient to boost walking speed. Interestingly, both loss and gain of function for *DNT-2* also
356 caused seizures (Figure S7). Thus, dopamine-dependent locomotion is regulated by the function of DNT-2,
357 Toll-6 and Kek-6.

358 Next, as dopamine is an essential neurotransmitter for learning and memory (Adel and Griffith
359 2021), we asked whether DNT-2 might influence appetitive olfactory conditioning. Starved flies were
360 trained to associate a sugar reward with an odour (CS+) while another odour was presented without sugar
361 (CS-), and their preference for CS+ versus CS- was measured, 24h after training (Tempel et al. 1983, Krashes
362 and Waddell 2008, 2011). Remarkably, over-expression of *DNT-2FL* in DNT-2 neurons in adults enhanced

363 appetitive long-term memory (Figure 6G), consistent with the positive role of DNT-2 in synaptogenesis that
364 we demonstrated above.
365 In summary, we have shown that alterations in DNT-2, Toll-6 and Kek-6 levels that caused
366 structural phenotypes in DANs also modified dopamine-dependent behaviours, locomotion and long-term
367 memory.
368
369 DISCUSSION
370 Our findings indicate that structural plasticity and degeneration in the brain are two manifestations of a
371 shared molecular mechanism that could be modulated by experience. Loss of function for *DNT-2, Toll-6* and
372 *kek-6* caused cell loss, affected arborisations and synaptogenesis in DANs and impaired locomotion;
373 neuronal activity increased DNT-2 production and cleavage and remodelled connecting DNT-2 and PAM
374 synapses; and over-expression of *DNT-2* increased TH levels, PAM cell number, dendrite complexity, and
375 synaptogenesis, and it enhanced locomotion and long-term memory.
376 It was remarkable to find that the number of dopaminergic neurons in the *Drosophila* adult brain is
377 plastic, and this is functionally relevant as it can influence behaviour. We showed that PAM cell number is
378 variables across individuals, that adult-specific gain of *DNT-2* function increases, whereas loss of *DNT-2* or
379 *Toll-6* function decreases, PAM cell number. Loss of *DNT-2* function in mutants, constant loss of *Toll-6*
380 function in DANS and adult-restricted knock-down of either *DNT-2* (in DNT-2 neurons) or *Toll-6* (in Toll-6
381 neurons and in DANs) all resulted in DAN cell loss, verified with three distinct reporters, and consistently
382 with the increase in DAN apoptosis. Furthermore, DAN cell loss in *DNT-2* mutants could be rescued by the
383 over-expression of *Toll-6* in DANs. Cell loss was also verified using two reporter types (ie GAL4 based
384 nuclear reporters and cytoplasmic anti-TH antibodies), multiple GAL4 drivers and mutants, and multiple cell
385 counting methods, including automatic cell counting with DeadEasy plug-ins for His-YFP and nls-Tomato
386 (where the signal was of high contrast and sphericity) and software assisted manual cell counting for anti-
387 TH (where the signal is more diffuse and less regular in shape). DeadEasy plug-ins have been used before
388 for reliably counting His-YFP labelled cells in both larval CNS and adult brains, including Kenyon cells (Kato

389 et al. 2011, Forero et al. 2012, Losada-Perez et al. 2016, Li et al. 2020, Harrison et al. 2021). Thus, the
390 finding that loss of *DNT-2* and *Toll-6* function in the adult brain cause dopaminergic neuron loss is robust.
391 Our findings are reminiscent of the increased apoptosis and cell loss in adult brains with *Toll-2* loss of
392 function (Li et al. 2020), and the support of DAN survival by Toll-1 and Toll-7 driven autophagy (Zhang et al.
393 2024). They are also consistent with a report that loss of function for *DNT-2* or *Toll-6* induced apoptosis in
394 the third instar larval optic lobes (McLaughlin et al. 2019). This did not result in neuronal loss - which was
395 interpreted as due to Toll-6 functions exclusive to glia (McLaughlin et al. 2019) - but instead of testing the
396 optic lobes, neurons of the larval abdominal ventral nerve cord (VNC) were monitored (McLaughlin et al.
397 2019). In the VNC, Toll-6 and -7 function redundantly and knock-down of both is required to cause neuronal
398 loss in embryos (McIlroy et al. 2013), whereas in L3 larvae and pupae the phenotype is compounded by
399 their pro-apoptotic functions (Foldi et al. 2017). It is crucial to consider that the DNT-Toll signalling system
400 can have distinct cellular outcomes depending on context, cell type and time, i.e. stage (Foldi et al. 2017, Li
401 et al. 2020, Li and Hidalgo 2021). Our work shows that in the adult *Drosophila* brain DAN neurons receive
402 secreted growth factors that maintain cellular integrity, and this impacts behaviour. Consistently with our
403 findings, *Drosophila* models of Parkinson's Disease reproduce the loss of DANs and locomotion impairment
404 of human patients (Feany and Bender 2000, Riemensperger et al. 2011, Riemensperger et al. 2013, Sun et
405 al. 2018). Dopamine is required for locomotion, associative reward learning and long-term memory
406 (Riemensperger et al. 2011, Riemensperger et al. 2013, Waddell 2013, Sun et al. 2018, Boto et al. 2020,
407 Adel and Griffith 2021). In *Drosophila*, this requires PAM, PPL1 and DAL neurons and their connections to
408 Kenyon Cells and MBONs (Heisenberg 2003, Chen et al. 2012, Placais et al. 2012, Aso et al. 2014b, Placais et
409 al. 2017, Boto et al. 2020, Adel and Griffith 2021, Huang et al. 2024). DNT-2 neurons are connected to all
410 these neuron types, which express *Toll-6* and *kek-6,* and modifying their levels affects locomotion and long-
411 term memory. Altogether, our data demonstrate that structural changes caused by altering DNT-2, Toll-6
412 and Kek-6 modified dopamine-dependent behaviours, providing a direct link between molecules, structural
413 circuit plasticity and behaviour.

414 We used neuronal activation as a proxy for experience, but the implication is that experience would
415 similarly drive the structural modification of circuits labelled by neuromodulators. Similar manipulations of
416 activity have previously revealed structural circuit modifications. For example, hyperpolarising olfactory
417 projection neurons increased microglomeruli number, active zone density and post-synaptic site size in the
418 calyx, whereas inhibition of synaptic vesicle release decreased the number of microglomeruli and active
419 zones (Kremer et al. 2010). There is also evidence that experience can modify circuits and behaviour in
420 *Drosophila.* For example, natural exposure to light and dark cycles maintains the structural homeostasis of
421 presynaptic sites in photoreceptor neurons, which breaks down in sustained exposure to light (Sugie et al.
422 2015). Prolonged odour exposure causes structural reduction at the antennal lobe and at the output pre-
423 synaptic sites in the calyx, and habituation (Devaud et al. 2001, Pech et al. 2015). Similarly, prolonged
424 exposure to CO2 caused a reduction in output responses at the lateral horn and habituation (Sachse et al.
425 2007). Our findings are also consistent with previous reports of structural plasticity during learning in
426 *Drosophila.* Hypocaloric food promotes structural plasticity in DANs, causing a reduction specifically in
427 connections between DANs and Kenyon cells involved in aversive learning, thus decreasing the memory of
428 the aversive experience (Coban et al. 2024). By contrast, after olfactory conditioning, appetitive long-term
429 memory increased axonal collaterals in projection neurons, and synapse number at Kenyon cell inputs in
430 the calyx (Baltruschat et al. 2021). Our data provide a direct link between a molecular mechanism, synapse
431 formation in a dopaminergic circuit and behavioural performance. Since behaviour is a source of
432 experience, the discovery that a neurotrophin can function with a Toll and a neuromodulator to sculpt
433 circuits provides a mechanistic basis for how experience can shape the brain throughout life.
434 Importantly, in humans structural brain plasticity (e.g. adult neurogenesis, neuronal survival,
435 neurite growth and synaptogenesis) correlates with anti-depressant treatment, learning, physical exercise
436 and well-being (Cotman and Berchtold 2002, Woollett and Maguire 2011, Castren and Monteggia 2021,
437 Cheng et al. 2022). Conversely, neurite, synapse and cell loss, correlate with ageing, neuroinflammation,
438 psychiatric and neurodegenerative conditions (Holtmaat and Svoboda 2009, Lu et al. 2013, Wohleb et al.
439 2016, Forrest et al. 2018, Vahid-Ansari and Albert 2021, Wang et al. 2022). Understanding how experience

440 drives the switch between generative and destructive cellular processes shaping the brain is critical to
441 understand brain function, in health and disease. In this context, the mechanism we have discovered could
442 also operate in the human brain. In fact, there is deep evolutionary conservation in DNT-2 vs mammalian
443 NT function (e.g. BDNF), but some details differ. Like mammalian NTs, full-length DNTs/Spz proteins contain
444 a signal peptide, an unstructured pro-domain and an evolutionarily conserved cystine-knot of the NT family
445 (Zhu et al. 2008, Arnot et al. 2010, Foldi et al. 2017). Cleavage of the pro-domain releases the mature
446 cystine-knot (CK). In mammals, full-length NTs have opposite functions to their cleaved forms (e.g.
447 apoptosis vs cell survival, respectively). However, DNT-2FL is cleaved by intracellular furins, and although
448 DNT-2 can be found both in full-length or cleaved forms in vivo, it is most abundantly found cleaved (Zhu et
449 al. 2008, McIlroy et al. 2013, Foldi et al. 2017). As a result, over-expressed *DNT-2FL* does not induce
450 apoptosis and instead it promotes cell survival (Foldi et al. 2017). The same functions are played by over-
451 expressed mature *DNT-2CK* as by *DNT-2FL* (Zhu et al. 2008, Foldi et al. 2017, Ulian-Benitez et al. 2017). In S2
452 cells, transfected DNT-2CK is not secreted, but when over-expressed in vivo it is functional (Zhu et al. 2008,
453 Foldi et al. 2017, Ulian-Benitez et al. 2017) (and this work). In fact, over-expressed *DNT-2CK* also maintains
454 neuronal survival, connectivity and synaptogenesis (Zhu et al. 2008, Foldi et al. 2017, Ulian-Benitez et al.
455 2017) (and this work). Similarly, over-expressed mature *spz-1-C106* can rescue the *spz-1*-null mutant
456 phenotype (Hu et al. 2004) and over-expressed *DNT-1CK* can promote neuronal survival, connectivity and
457 rescue the *DNT-1* mutant phenotype (Zhu et al. 2008). Consistently, both DNT-2FL and DNT-2CK have
458 neuro-protective functions promoting cell survival, neurite growth and synaptogenesis (Zhu et al. 2008,
459 Sutcliffe et al. 2013, Foldi et al. 2017, Ulian-Benitez et al. 2017) (and this work). Importantly, over-
460 expressing *DNT-2FL* enables to investigate non-autonomous functions of DNT-2 (Ulian-Benitez et al. 2017).
461 We have shown that *DNT-2FL* can induce synaptogenesis non-autonomously in target neurons. Similarly,
462 DNT-2 is a retrograde factor at the larval NMJ, where transcripts are located post-synaptically in the
463 muscle, DNT-2FL-GFP is taken up from muscle by motoneurons, where it induces synaptogenesis (Sutcliffe
464 et al. 2013, Ulian-Benitez et al. 2017). Importantly, we have shown that neuronal activity increased
465 production of tagged DNT-2-GFP, and its cleavage. In mammals, neuronal activity induces synthesis, release

466 and cleavage of BDNF, leading to neuronal survival, dendrite growth and branching, synaptogenesis and
467 synaptic plasticity (ie LTP)(Poo 2001, Horch and Katz 2002, Lu et al. 2005, Arikkath 2012, Wang et al. 2022).
468 Like BDNF, DNT-2 also induced synaptogenesis and increased bouton size.

469 It may not always be possible to disentangle primary from compensatory phenotypes, as Hebbian,
470 homeostatic and heterosynaptic plasticity can concur (Forrest et al. 2018, Jenks et al. 2021). Mammalian
471 BDNF increases synapse number, spine size and long-term potentiation (LTP), but it can also regulate
472 homeostatic plasticity and long-term depression (LTD), depending on timing, levels and site of action (Poo
473 2001, Lu et al. 2005, Wang et al. 2022). In this context, neuronal stimulation of DNT-2 neurons induced
474 synapse formation in PAM neuron SMP dendrites, whereas DNT-2 over-expression from DNT-2 neurons
475 increased synapse size at SMP and synapse number in PAM outputs at the mushroom body lobes. These
476 distinct effects could be due to the combination of plasticity mechanisms and range of action. Neuronal
477 activity can induce localised protein synthesis that facilitates local synaptogenesis and stabilises emerging
478 synapses (Forrest et al. 2018). By contrast, DNT-2 induced signalling via the nucleus can facilitate
479 synaptogenesis at longer distances, in output sites. In any case, synaptic remodelling is the result of
480 concurring forms of activity-dependent plasticity altogether leading to modification in connectivity patterns
481 (Forrest et al. 2018, Jenks et al. 2021). Long-term memory requires synaptogenesis, and in mammals this
482 depends on BDNF, and its role in the protein-synthesis dependent phase of LTP (Poo 2001, Minichiello
483 2009, Wang et al. 2022). BDNF localised translation, expression and release are induced to enable long-
484 term memory (Poo 2001, Lee et al. 2004, Minichiello 2009, Wang et al. 2022). We have shown that
485 similarly, over-expressed *DNT-2FL* increased both synaptogenesis in sites involved in reward learning, and
486 long-term memory after appetitive conditioning.

487 The relationship of NTs with dopamine is also conserved. DNT-2 and DAN neurons form
488 bidirectional connectivity that modulates both DNT-2 and dopamine levels. Similarly, mammalian NTs also
489 promote dopamine release and the expression of DA receptors (Blochl and Sirrenberg 1996, Guillin et al.
490 2001). Furthermore, DAN cell survival is maintained by DNT-2 in *Drosophila,* and similarly DAN cell survival
491 is also maintained by NT signalling in mammals and fish (Hyman et al. 1991, Sahu et al. 2019). Importantly,

492 we showed that activating DNT-2 neurons increased the levels and cleavage of DNT-2, up-regulated DNT-2
493 increased *TH* expression, and this initial amplification resulted in the inhibition of cAMP signalling via the
494 dopamine receptor Dop2R in DNT-2 neurons. This negative feedback could drive a homeostatic reset of
495 both DNT-2 and dopamine levels, important for normal brain function. In fact, we showed that alterations
496 in DNT-2 levels could cause seizures. Importantly, alterations in both NTs and dopamine underlie many
497 psychiatric disorders and neurodegenerative diseases in humans (Hyman et al. 1991, Guillin et al. 2001,
498 Berton et al. 2006, Forrest et al. 2018, Wang et al. 2022).

499 We have uncovered a novel mechanism of structural brain plasticity, involving a NT ligand
500 functioning via a Toll and a kinase-less Trk-family receptor in the adult *Drosophila* brain. Toll receptors in
501 the CNS can function via ligand dependent and ligand-independent mechanisms (Anthoney et al. 2018).
502 However, in the context analysed, Toll-6 and Kek-6 function in structural circuit plasticity depends on their
503 ligand DNT-2. This is also consistent with their functions promoting axonal arbour growth, branching and
504 synaptogenesis at the NMJ (Ulian-Benitez et al. 2017). Furthermore, Toll-2 is also neuro-protective in the
505 adult fly brain, and loss of *Toll-2* function caused neurodegeneration and impaired behaviour (Li et al.
506 2020). There are six *spz/DNT*, nine *Toll* and six *kek* paralogous genes in *Drosophila* (Tauszig et al. 2000,
507 MacLaren et al. 2004, Mandai et al. 2009, Ulian-Benitez et al. 2017), and at least seven *Tolls* and three
508 adaptors are expressed in distinct but overlapping patterns in the brain (Li et al. 2020). Such combinatorial
509 complexity opens the possibility for a fine-tuned regulation of structural circuit plasticity and homeostasis
510 in the brain.

511 *Drosophila* and mammalian NTs may have evolved to use different receptor types to elicit
512 equivalent cellular outcomes. In fact, in mammals, NTs function via Trk, $p75^{NTR}$ and Sortilin receptors, to
513 activate ERK, PI3K, NFκB, JNK and CaMKII (Lu et al. 2005, Wang et al. 2022). Similarly, DNTs with Tolls and
514 Keks also activate ERK, NFκB, JNK and CaMKII in the *Drosophila* CNS (McIlroy et al. 2013, Foldi et al. 2017,
515 Ulian-Benitez et al. 2017, Anthoney et al. 2018). However, alternatively, NTs may also use further receptors
516 in mammals. Trks have many kinase-less isoforms, and understanding of their function is limited (Fryer et
517 al. 1996, Stoilov et al. 2002). They can function as ligand sinks and dominant negative forms, but they can

518 also function independently of full-length Trks to influence calcium levels, growth cone extension and
519 dendritic growth and are linked to psychiatric disorders, e.g. depression (Ferrer et al. 1999, Yacoubian and
520 Lo 2000, Ohira et al. 2006, Carim-Todd et al. 2009, Ernst et al. 2009, Ohira and Hayashi 2009, Fenner 2012,
521 Tessarollo and Yanpallewar 2022). Like Keks, perhaps kinase-less Trks could regulate brain plasticity vs.
522 degeneration.

523 A functional relationship between NTs and TLRs could exist also in humans, as in cell culture,
524 human BDNF and NGF can induce signalling from a TLR (Foldi et al. 2017) and NGF also functions in
525 immunity and neuroinflammation (Levi-Montalcini et al. 1996, Hepburn et al. 2014). Importantly, TLRs can
526 regulate cell survival, death and proliferation, neurogenesis, neurite growth and collapse, learning and
527 memory (Okun et al. 2011). They are linked to neuroinflammation, psychiatric disorders,
528 neurodegenerative diseases and stroke (Okun et al. 2011, Figueroa-Hall et al. 2020, Adhikarla et al. 2021).
529 Intriguingly, genome-wide association studies (GWAS) have revealed the involvement of TLRs in various
530 brain conditions and potential links between NTs and TLRs in, for example, major depression (Sharma 2012,
531 Mehta et al. 2018, Chan et al. 2020, Garrett et al. 2021). Importantly, alterations in NT function underlie
532 psychiatric, neurologic and neurodegenerative brain diseases (Lu et al. 2005, Martinowich et al. 2007,
533 Krishnan and Nestler 2008, Lu et al. 2013, Park and Poo 2013, Wohleb et al. 2016, Yang et al. 2020,
534 Casarotto et al. 2021, Wang et al. 2022) and BDNF underlies the plasticity inducing function of anti-
535 depressants (Lu et al. 2013, Casarotto et al. 2021, Wang et al. 2022). It is compelling to find out whether
536 and how these important protein families – NTs, TLRs and kinase-less Trks - interact in the human brain.
537

538 **Conclusion**

539 To conclude, we provide a direct link between structural circuit plasticity and behavioural performance, by
540 a novel molecular mechanism. The neurotrophin DNT-2 and its receptors Toll-6 and the kinase-less Trk
541 family Kek-6 are linked to a dopaminergic circuit. Neuronal activity boosts DNT-2, and DNT-2 and dopamine
542 regulate each other homeostatically. Dopamine labels the circuits engaged and DNT-2, a growth factor,
543 with its receptors Toll-6 and Kek-6, drives structural plasticity in these circuits, enhancing dopamine-

544 dependent behavioural performance. These findings mean that DNT-2 is a plasticity factor in the *Drosophila*
545 brain, that could enable experience-dependent behavioural enhancement. Whether NTs can similarly
546 functions with TLRs and Kinase-less Trks remains to be explored. As behaviour is a source of experience,
547 this has profound implications for understanding brain function and health.
548

549 ACKNOWLEDGEMENTS

550 We thank our lab, Carolina Rezaval and Thomas Riemensperger for comments on the manuscript; Carolina
551 Rezaval, Reinhard Wolf, Martin Heisenberg and Scott Waddell for advice on - Karina Piotrowska for help
552 with - behaviour experiments; Xiufeng Li for help with programming; Serge Birman, Ann-Shyn Chiang, Ron
553 Davis, André Fialá, Barret Pfeiffer, Xi Rao, Carolina Rezaval, Iris Salecker for flies; DSHB (Iowa) for
554 antibodies; AddGene for plasmids; Bloomington Stock Centre for *Drosophila* stocks. This work was funded
555 by Marie-Curie Sklodowska Post-Doctoral fellowship to J.S.; Science Without Borders-CAPES PhD
556 Studentship BEX 13380/13-3 to SUB; BBSRC Project Grants BB/R00871X/1 and BB/P004997/1 to A.H.; and
557 Wellcome Trust Investigator Award 223197/Z/21/Z to A.H.
558

559 AUTHOR CONTRIBUTIONS

560 J.S., V.C and A.H. designed and/or executed experiments and/or analysed data; S.U-B, G.L, D.S, X.W., F.R.C,
561 M.M. executed experiments and analysed data; M.G.F, S.C., A.H. developed tools; D.K., G.J, V.C., A.H.
562 supervised; J.S and A.H. wrote the manuscript. A.H. conceived and directed the project. All authors
563 provided feedback on, and contributed to improvements to, the manuscript.
564

565 DATA AVAILABILITY STATEMENT

566 All data are contained within the manuscript; metadata and statistical analysis details including full
567 genotypes, sample sizes, statistical tests and p values have been provided in Table S2. This work generated
568 fly stocks and molecular constructs, which we will distribute on request. Raw data will be distributed on
569 request.

570

571 DECLARATION OF INTERESTS

572 The authors declare that they have no conflict of interest.
573
574
575 MATERIALS AND METHODS

576 **Genetics**

577 **Mutants:** *DNT2*[37] and *DNT2*[18] are protein null(Foldi et al. 2017, Ulian-Benitez et al. 2017). *Toll6*[31] is a null

578 mutant allele(McIlroy et al. 2013). **Driver lines:** *DNT2-Gal4* is a CRISPR/Cas9-knock-in allele, with GAL4 at

579 the start of the gene (this work, see below). *Toll-6-Gal4* was generated by RMCE from *MIMIC Toll-6*[MIO2127]*;*

580 *kek6-Gal4* from *MIMIC Kek6*[MI12953](Ulian-Benitez et al. 2017, Li et al. 2020). *MB320C-Gal4 (BSC68253),*

581 *MB301B-Gal4 (BSC68311), R58E02-Gal4 (BSC41347), MB247-Gal80 (BSC64306), R58E02-LexA (BSC52740),*

582 *R14C08-LexA (BSC52473)* were from the *Drosophila* Bloomington Stock Centre (BSC). *Dop1R2-LexA, Dop2R-*

583 *LexA, Gad-LexA* were kindly provided by Yi Rao; *TH-LexA* (gift of Ron Davis), *TH-Gal4,R58E02-GAL4* (gift of

584 Serge Birman); *G0431-Gal4 (DAL-GAL4), VT49239 nls LexA (DAL LexA)* (gifts from Ann-Shyn Chiang);

585 tubGal80ts, Tdc-LexA. **Reporter lines:** *UAS-CD8::GFP,* for membrane tethered GFP; *UAS-histone-YFP*, for

586 YFP-tagged nuclear histone; *UASFlybow1.1*, constant membrane tethered expression (gift of Iris Salecker);

587 *13xLexAop-nls-tdTomato,* nuclear Tomato (gift of B. Pfeiffer); *UASCD8::RFP, LexAopCD8::GFP* (BSC32229),

588 for dual binary expression; *UAS-homer-GCaMP* for post-synaptic densities (gift of André Fialá), *UAS-*

589 *syt.eGFP* (BSC6925) and *LexAop-Syt-GCaMP* (BSC64413) for presynaptic sites. **For connectivity*:*** *UAS-*

590 *DenMarkRFP, UAS-Dsyd1GFP* (gift of Carolina Rezaval); TransTango: *yw UAS-myrGFP,QUAS-mtdTomato-*

591 *3xHA attP8; Trans-Tango@attP40* (BSC77124); BAcTrace 806 *(w;LexAop2-Syb::GFP-P10(VK37) LexAop-*

592 *QF2::SNAP25::HIVNES::Syntaxin(VK18)/CyO; UAS-B3Recombinase (attP2) UAS<B3Stop<BoNT/A (VK5)*

593 *UAS<B3Stop<BoNT/A(VK27) QUAS-mtdTomato::HA/TM2*): **MCFO clones**: *hs-FLPG5.PEST;; 10xUAS*

594 *(FRT.stop) myr::smGdP-OLLAS 10xUAS (FRT.stop) myr::smGdP-HA 10xUAS (FRT.stop) myr::smGdP-V5-THS-*

595 *10xUAS (FRT.stop) myr::smGdP-FLAG* (BSC64086). **Optogenetic activation:** *20x UAS-V5-Syn-CsChrimson td*

596 *tomato* (gift of B. Pfeiffer**). For thermogenetic activation:** *UASTrpA1@attP2 (BSC26264)* and *UAS-*

597 *TrpA1@attP216 (BSC26263).* **UAS gene over-expression**: *UAS-DNT2CK, UAS-DNT2FL-GFP, UAS-DNT2-FL-*
598 *47C, UAS-Toll-6^{CY}*(McIlroy et al. 2013, Foldi et al. 2017). **UAS-RNAi knockdown:** *UAS-DNT2RNAi*
599 (VDRC49195), *UAS-Toll6RNAi* (VDRC928), *y^1v^1; UAS-Toll6RNAi[Trip.HMS04251]* (BSC 56048*), UAS-kek6RNAi*
600 (VDCR 109681), *y^1v^1; UAS-Dop2R-RNAi[TRiP.HMC02988](*BSC50621).
601
602 **Molecular biology**
603 *DNT-2GAL4* was generated by CRISPR/Cas9 enhanced homologous recombination. 1 kb long 5' and 3'
604 homology arms (HA) were amplified by PCR from genomic DNA of wild type flies, using primers for 5'HA:
605 atcgcaccggtttttacaggcaccccatgtctga containing AgeI cutting site and
606 cttgacgcggccgcTGTCAATTCATTCGCCGTCGAT containing NotI cutting site. 3'HA primers were:
607 tattaggcgcgccATGACAAAAAGTATTAAACGTCCGCCC containing AscI cutting site and
608 tactcgactagtgaagcacacccaaaatacccagg containing SpeI cutting site. HAs were sequentially cloned by
609 conventional cloning into pGEM-T2AGal4 vector (Addgene #62894). For gRNA cloning, two 20 nucleotide
610 gRNA oligos (gtcGACAAGTTCTTCTTACCTATG and aaacCATAGGTAAGAAGAACTTGTC) were designed using
611 Optimal Target Finder. BbsI enzyme sites were added: gtc(g) at the 5' end of sense oligo, and aaac at the 5'
612 end of the antisense oligo. gRNA is located at 41 bp downstream of the start codon of DNT-2 within the
613 first coding exon. The gRNA was cloned into pU6.3 using conventional ligation. The two constructs were
614 injected in Cas9 bearing flies and red fluorescent (3xP3-RFP) transformants were selected and balanced,
615 after which 3xP3-RFP was removed with CRE-recombinase.
616
617 **qRT-PCR**
618 qRT-PCR was carried out from 20 whole adult fruit-fly heads, frozen in liquid nitrogen before homogenising
619 in 50 ml Trizol (Ambion #AM9738), followed by a stand RNA extraction protocol. RNA was treated with
620 DNase treatment (ThermoFisher # AM1906) to remove genomic DNA. 200 ng of RNA was used for cDNA
621 synthesis following Goscript Reverse Transcriptase (Promega #237815) protocol. Sample was diluted 1:4
622 with Nuclease free H_2O. Standard qPCR was performed with SensiFast syb Green Mix (Bioline #B2092020)

623 in ABI qPCR plate (GeneFlow #P3-0292) and machine. To amplify TH mRNA the following primers were
624 used: TH-F: CGAGGACGAGATTTTGTTGGC and TH-R: TTGAGGCGGACCACCAAAG. GAPDH was used as a
625 housekeeping control. Reactions were performed in triplicate. Specificity and size of amplification products
626 were assessed by melting curve analyses. Target gene expression relative to reference gene is expressed as
627 value of $2^{-\Delta\Delta Ct}$ (where Ct is the crossing threshold).
628
629 **Conditional expression**
630 **Multiple Colour Flip Out clones:** *DNT2-Gal4, Toll6-Gal4* and *kek6-Gal4* were crossed with
631 *hsFLP::PEST;;MCFO* flies, female offspring were collected and heat-shocked at 37°C in a water bath for 15
632 mins, then kept for 48h at 25°C before dissecting their brains. ***TransTango:*** DNT2-Gal4 or Oregon female
633 virgins were crossed with *TransTango* males, progeny flies were raised at 18°C constantly and 15 days after
634 eclosion, female flies were selected for immunostaining. **Thermogenetic activation with *TrpA1:*** Fruit-flies
635 were bred at 18°C from egg laying to 4 days post-adult eclosion, then shifted to 29°C in a water bath for
636 24h followed by 24h recovery at room temperature for over-expressed *DNT-2FL-GFP*; for the other
637 experiments, after breeding as above, adult flies were transferred to an incubator at 30°C, kept there for
638 24h and then brains were dissected. **Conditional gene over-expression and RNAi knockdown:** Flies bearing
639 the temperature sensitive GAL4 repressor tubGal80^{ts} were kept at 18°C from egg laying to adult eclosion,
640 then transferred to 30 °C incubator for 48h for Dcp-1+ and cell counting experiments and for 120h for TH+
641 cell counting.
642
643 **Immunostainings**
644 Adult fruit-fly female brains were dissected (in PBS), fixed (in 4% para-formaldehyde, room temperature,
645 20-30min) and stained following standard protocols. Primary antibodies and their dilutions were as follows:
646 Mouse anti-Brp (nc82) 1:10 (DSHB); Rabbit anti-GFP 1:250 (Thermofisher); Mouse anti-GFP 1:250
647 (Thermofisher); Chicken anti-GFP 1:500 (Aves); Rabbit anti-FLAG 1:50 (Sigma); Mouse anti-V5 1:50
648 (Invitrogen); Chicken anti-HA 1:50 (Aves); Rabbit anti-VGlut 1:500 (gift of Hermann); Mouse anti-TH 1:250

649 (Immunostar); Rabbit anti-TH 1:250 (Novus Biologicals); Rabbit anti-DsRed 1:250 (Clontek); Mouse anti-
650 ChAT4B1 1:250 (DSHB); Rabbit anti-5-HT 1:500 (Immunostar); Rabbit Anti-DCP-1 1:250 (Cell Signalling).
651 Seconday antibodies were all used at 1:500 and all were from Thermofisher: Alexa Flour 488 Goat anti-
652 mouse, Alexa Flour 488 donkey anti-rabbit, Alexa Flour 488 Goat anti-rabbit (Fab')2, Alexa Flour 488 Goat
653 anti-chicken, Alexa Four 546 Goat anti-rabbit, Alexa Four 546 Goat anti-mouse, Alex Four 647 Goat anti-
654 rabbit, Alex Four 647 Goat anti-mouse.
655
656 **Microscopy and Imaging**
657 **Laser scanning confocal microscopy.** Stacks of microscopy images were acquired using laser scanning
658 confocal microscopy with either Zeiss LSM710, 900 or Leica SP8. Brains were scanned with a resolution of
659 1024x1024, with Leica SP8 20x oil objective and 1 mm step for whole brain and DCP-1 stainings, 40x oil
660 objective and 1 mm step for central brain. Resolution of 1024x512 was used for analysing PAM clusters
661 with 0.96 mm step for cell counting; 0.5 mm step for neuronal morphology; and 63x oil objective with
662 0.5mm step for neuronal connections. Acquisition speed in Leica SP8 was 400Hz, with no line averaging.
663 Resolution of 3072x3072 was used for single image analysis of synapses, using either Leica SP8 or Zeiss
664 LSM900 and Airyscan acquisition with 40x water objective speed 6, and average 4, or with 1024x512, with
665 40x oil lens 2x zoom and 0.35mm step. TH counting in PAM were scanned with Zeiss 710 with a resolution
666 1024x1024, 40x oil objective, step 1 mm, speed 8. Zeiss LSM900 Airyscan with a resolution of 1024x1024,
667 40x water objective, speed 7, 0.7 zoom and 0.31µm step size was used for acquisition of optical sections of
668 synapses in PAM neurons.
669 **Optogenetics and Epac1 FRET 2-photon imaging**
670 To test whether DNT-2 neurons can respond to dopamine via the Dop2R inhibitory receptor, we used the
671 cAMP sensor Epac1 and 2-photon confocal microscopy. Epac1 is FRET probe, whereby data are acquired
672 from CFP and YFP emission and lower YFP/CFP ratio reveals higher cAMP levels. DNT-2Gal4 flies were
673 crossed to *UAS-CsChrimson UAS Epac1* flies, to stimulate DNT-2 neurons and detect cAMP levels in DNT2
674 neurons. 1-3 day-old *DNT2Gal4>UASCsChrimson, UAS Epac1* flies were collected and separated in two

675 groups. Flies bearing *DNT2Gal4 UASCsChrimson UAS Epac1 UASDop2RRNAi* were fed on 50μM all-trans
676 retinal food for at least 3 days prior to imaging and kept in constant darkness prior to the experiment.
677 Optogenetic stimulation of fly brains expressing CsChrimson in DNT-2 neurons was carried out
678 using a sapphire 588nm laser, in a 2-photon confocal microscope. For acquisition of YFP and CFP data from
679 Epac1 samples, a FV30-FYC filter was applied, using a 925nm laser for both YFP and CFP imaging. The
680 stimulation laser was targeted onto DNT-2 neuron projections in SMP region for 20s. Acquisition ROI was at
681 DNT-2A cell bodies with a frame rate of around 10Hz. The first acquisition started 10s before the 20s
682 stimulation and consequential acquisition was done every 30s for 10 cycles.
683 Image analysis of Epac data was carried out using ImageJ. The two channels (YFP and CFP) were
684 separated, and the ratio of YFP/CFP for each pixel was calculated using the ImageJ>Image Calculator by
685 diving YFP channel by CFP channel. The obtained result of YFP/CFP ratio was saved and the mean ratio of
686 YFP/CFP in the ROI was calculated for each time point and 11 time points were used. The 11 values
687 represent the ratio of YFP/CFP change in the cell body upon stimulation, with 30s interval and repeated 10
688 times.
689 **Cell counting:** To count cells labelled with nuclear reporters (e.g. Histone-YFP, nls-tdTomato) and Dcp-1+
690 cells, where signal is of high intensity, contrast and sphericity, we adapted the DeadEasy Central Brain
691 ImageJ plug-in (Li et al. 2020) for automatic cell counting in adult brains. DeadEasy plug-ins automatically
692 identify and count cells labelled with nuclear reporters in 3D stacks of confocal image in the nervous
693 system of embryos (Forero et al. 2010a, Forero et al. 2010b), larvae (Kato et al. 2011, Forero et al. 2012,
694 Losada-Perez et al. 2016, Harrison et al. 2021) and adult (Li et al. 2020) *Drosophila*. DeadEasy plug-ins are
695 accurate at counting cells sparsely labelled with nuclear markers, and importantly, treat all genotypes
696 objectively and equally yielding reliable data. Here, adult brains expressing Histone-YFP or nls-td-tomato
697 reporters were dissected, fixed and scanned without staining them. DeadEasy Central Brain was used with
698 threshold set to 75.
699 To count the TH labelled PAMs, where both the signal and the labelled-cell shape are more
700 irregular, we used assisted manual cell counting using two methods. First, we developed a plug-in called

701 DeadEasy DAN as follows. A median filter was used to reduce Poison noise, without having large losses at
702 the edges. Then, a 3D morphological closing was performed. Next, all very dark pixels were assigned a value
703 of zero. To mark each cell, each chasm in the image was found using a 3D extended h-minimal transform.
704 As more than one local minimum can be found within each cell, which would result in counting a cell
705 multiple times, a 3D inverse dome detection was performed, and then labelled. Thus, each inverse dome
706 was used as a seed to identify each cell. Once the seeds were obtained, a 3D watershed transformation was
707 performed to recover the shape of the cells. Then, we ran DeadEasy DAN on our raw data, to obtain a
708 results stack of images and formed a merged stack between the raw and result stacks, to manually add any
709 missing cells. This assisted cell counting method was effective at producing accurate cell counts with less
710 labour and time than conventional manual counting and worked well for some genotypes (Figure 3D).
711 However, it was less effective with RNAi knock-down genotypes, where the signal can be less intense, for
712 which TH+ cells were counted manually, assisted by the ImageJ cell counter instead.
713 **Dendrite analysis with Imaris:** To analyze dendritic complexity, image data were processed with Imaris
714 using the "Filaments" module with the default algorithm and "Autopatch function". A simple region of
715 interest (ROI) with parallelepiped shape was delimited. Thresholds were set for the largest and the
716 smallest diameter of the dendrite, and this was consistent across samples within the same experiment. The
717 starting point threshold was adjusted to only represent the soma of the neurons, and the "Seed Points
718 threshold" to match the branches of the neurons. "Remove Seed Points Around Starting Points" and
719 "Remove Disconnected Segments" were chosen, keeping the default values. The threshold for background
720 substation and local contrast was consistent across all samples within an experiment. The "Edit function"
721 within the Filaments module was used to correct any inaccuracy detected in the resulting tracing. Number
722 of dendritic branches, dendritic segments, dendritic branch points and dendritic terminal points were
723 collected to compare differences between the groups.
724 **Vesicles, synapses and PSD analysis with Imaris:** To analyse the number and volume of Homer-GCaMP
725 GFP+ post-synaptic densities (PSD), Syt-GCaMP GFP+ presynaptic sites and DNT-2FLGFP+ vesicles, optical
726 section images of confocal stacks through the brain were processed with the Imaris "Spot function". To

727 analyze the number and volume of Homer-GCaMP GFP+ post-synaptic densities (PSD), the "Surface
728 module" from Imaris was used to restrict a region of interest (ROI). Then, "Absolute Intensity Thresholding"
729 method was applied to each sample choosing the same cutoff each time. The resulting surface was applied
730 to mask the original scan. The masked image was processed using "Image Processing module" from Imaris.
731 Background subtraction followed by threshold cutoff filters were applied. Afterwards, the "Spots module"
732 was used as explained below.

733 An ROI was determined for Syt-GCaMP GFP+ presynaptic sites and DNT-2FLGFP+ vesicles using the
734 "Surface module" with the "Edit Manually" option "Algorithm". The ROI for the SMP region started in the
735 slide immediately after the last slide where the soma of PAM neurons was detectable, and finished in the
736 last one where the dendrite was visible. The SMP region laterally was delimited by the black space given by
737 the α lobe position. For the MB lobe region, the ROI started in the first slide where γ5,β'2 and β2 was
738 visible (Aso et al., 2014) and finished in the last slide where this structure was appreciable. The surface was
739 used to create a "Masked Channel", which a posteriori was used to determine the spots using the Spots
740 module.

741 The "Spots module" algorithm was set to "Different Spot Sizes". An Estimated XY Diameter was set
742 according to each experiment group, using the same within an experiment. "Background Subtraction"
743 option was selected. "Intensity Center Filter" was used. "Spot Region" type was determined from "Local
744 Contrast", and the "Region Threshold" according to the "Region Border". Setting of the threshold was
745 consistent across genotypes.

746

747 **Behaviour**

748 **1. Startle induced negative geotaxis Assay** was carried out as described in (Sun et al. 2018). Groups of
749 approximately 10 male flies of the same genotype were placed in a fresh tube one night before the test,
750 after which flies were transferred to a column formed with two empty tubes 15cm long and 2cm and then
751 habituated for 30mins. Columns were tapped 3-4 times, flies fell to the bottom and then climbed upwards.
752 Multiple rounds of testing were performed 3-7 times in a row per column. The process was filmed and films

753 were analysed. Flies were scored during the first 15s after the tapping, and those that climbed above 13cm
754 and those that climbed below 2cm were counted separately. Results given are mean ± SEM of the scores
755 obtained with ten groups of flies per genotype. The performance index (PI) is defined as 1⁄2[(ntot + ntop −
756 nbot)/ntot], where ntot, ntop, and nbot are the total number of flies, the number of flies at the top, and
757 the number of flies at the bottom, respectively. The assay was carried out at 25°C, 55% humidity. Flies with
758 tubGal80^{ts} to conditionally overexpress or knock-down were shifted from 18 to 30°at eclosion and kept for
759 5 days at 30°C to induce Gal4. Experiments were carried in an environmental chamber at 31°C, 60%
760 humidity or in a humidity and temperature-controlled behaviour lab always kept at 25°C.
761 **2. Spontaneous Locomotion in an open arena:** Male flies of each genotype were collected and kept in groups
762 of 10-20 flies, in vials containing fresh fly food for 5-9 days. Before filming, three male flies from one genotype
763 were transferred into a 24 mm well of a multi-well plate using an aspirator and habituated for 15 – 20 mins.
764 The multi-well plate with transparent lid and bottom was placed on a white LED light pad (XIAOSTAR Light
765 Box) and either inside a light-shielding black box (PULUZ, 40*40*40cm) in a room with constant temperature
766 (25°C) and humidity (55%) to maintain stable environmental conditions (Figure 7D), or inside a temperature
767 controlled environmental chamber at 18°C or 30°C (Figure 7E,F,) . The locomotion behaviour of freely-moving
768 flies was filmed with a camera (Panasonic, HC-V260) in the morning from ZT1-ZT4 and for 10 min at a frame-
769 rate of 25 fps. The 10-min videos were trimmed (from 00:02:00 to 00:07:00) to 5-min videos for analysis using
770 Flytracker software(Eyjolfsdottir et al. 2014). For the *DNT-2* mutants and over-expression of Toll-6^{CY}
771 experiments, flies were bred and tested at 25 °C. To test over-expression of *DNT-2* with *tubGAL80^{ts}; DNT2-*
772 *Gal4>UAS-DNT-2FL*, flies were raised at 18°C until eclosion, and controls were kept and tested at 18°C; test
773 groups were transferred directly after eclosion to 30°C for 5 days and were tested in an environmental
774 chamber kept at 30°C, 60%. For thermo-genetic activation of DNT2 neurons using TrpA1 (DNT-
775 2GAL4>UASTrpA1), flies were bred at 18°C and kept at 18°C for 7-9 days post-eclosion. Following habituation
776 at 18°c for 20 mins in the multi-well plates, they were transferred to the 30°C chamber 10 mins before filming
777 to activate TrpA1 and then filmed for the following 10 minutes. Fly locomotion activity was tracked using
778 FlyTracker and calculated (distance and speed) in Matlab(Eyjolfsdottir et al. 2014) using the raw data

779 generated from the tracking procedure. The "walking distance" was calculated as the sum of the distance
780 flies moved and the "walking speed" was the speed of flies only when they were walking, and it was
781 calculated using only frames where flies moved above 4 mm/s (which corresponds to two body lengths).
782 **3. Appetitive long term memory test:** Appetitive long-term memory was tested as described in Krashes and
783 Waddell(Krashes and Waddell 2011). The two conditioning odours used were isoamyl acetate, Sigma-Aldrich
784 #24900822, 6mL in 8mL mineral oil (Sigma-Aldrich #330760) and 4-methylcyclohexanol (Sigma-Aldrich #
785 153095, 10mL in 8mL mineral oil). Groups of 80-120 mixed sex flies were starved in a 1% agar tube filled with
786 a damp 20 x 60 mm piece of filter paper for 18-20 hour before conditioning. During conditioning training,
787 one odorant was presented with a dry filter paper (unconditioned odour, CS-) for 2 minutes, before a 30
788 second break, and presentation of a second odorant with filter paper coated with dry sucrose (conditioned
789 odour, CS+). The test was repeated pairing the other odorant with sucrose, with a different group of flies to
790 form one replicate. After training, flies were transferred back to agar tubes for testing 24 hours later.
791 Performance index (PI) was calculated in the same way as in Krashes and Waddell(Krashes and Waddell
792 2011), as the number of flies approaching the conditioned odour minus the number of flies going in the
793 opposite direction, divided by the total number of flies. A single PI values is the average score from the test
794 with the reverse conditioning odour combination. Groups for which the total number of flies among both
795 odorants was below 15 were discarded. For the *DNT-2* over-expression experiments with *tubGAL80^{ts}; DNT-*
796 *2>DNT-2FL,* flies were raised at 18°C until 7-9 days post-eclosion. They were then either transferred to and
797 maintained at 23°C (controls) or 30°C for 18-20h starvation, training, and up to testing 24h later.
798 **Statistical analysis:** Statistical analyses were carried out using Graph-Pad Prism. Confidence interval was
799 95%, setting significance at $p<0.05$. Chi-square tests were carried out when comparing categorical data.
800 Numerical data were tested first for their type of distributions. If data were distributed normally, unpaired
801 Student t-tests were used to compare means between two groups and One Way ANOVA or Welch ANOVA
802 for larger groups, followed by post-doc Dunnett test for multiple comparisons to a fixed control. Two Way
803 ANOVA was used when comparisons to two variables were made. If data were not normally distributed,
804 non-parametric Mann-Whitney U-test for 2 two group comparisons and Kruskal Wallis ANOVA for larger

805 groups, followed by post-hoc Dunn's multiple comparisons test to a fixed control. Statistical details

806 including full genotypes, sample sizes, tests and p values are provided in Supplementary Table S2.

807

808 **REFERENCES**

809 Adel, M. and L. C. Griffith (2021). "The Role of Dopamine in Associative Learning in Drosophila: An
810 Updated Unified Model." *Neurosci Bull* **37**(6): 831-852.

811 Adhikarla, S. V., N. K. Jha, V. K. Goswami, A. Sharma, A. Bhardwaj, A. Dey, C. Villa, Y. Kumar and S. K.
812 Jha (2021). "TLR-Mediated Signal Transduction and Neurodegenerative Disorders." *Brain Sci* **11**(11).

813 Anthoney, N., I. Foldi and A. Hidalgo (2018). "Toll and Toll-like receptor signalling in development."
814 *Development* **145**(9).

815 Arikkath, J. (2012). "Molecular mechanisms of dendrite morphogenesis." *Front Cell Neurosci* **6**: 61.

816 Arnot, C. J., N. J. Gay and M. Gangloff (2010). "Molecular mechanism that induces activation of
817 Spatzle, the ligand for the Drosophila Toll receptor." *J Biol Chem* **285**(25): 19502-19509.

818 Aso, Y., D. Hattori, Y. Yu, R. M. Johnston, N. A. Iyer, T. T. Ngo, H. Dionne, L. F. Abbott, R. Axel, H.
819 Tanimoto and G. M. Rubin (2014a). "The neuronal architecture of the mushroom body provides a
820 logic for associative learning." *Elife* **3**: e04577.

821 Aso, Y., A. Herb, M. Ogueta, I. Siwanowicz, T. Templier, A. B. Friedrich, K. Ito, H. Scholz and H.
822 Tanimoto (2012). "Three dopamine pathways induce aversive odor memories with different
823 stability." *PLoS Genet* **8**(7): e1002768.

824 Aso, Y., D. Sitaraman, T. Ichinose, K. R. Kaun, K. Vogt, G. Belliart-Guerin, P. Y. Placais, A. A. Robie, N.
825 Yamagata, C. Schnaitmann, W. J. Rowell, R. M. Johnston, T. T. Ngo, N. Chen, W. Korff, M. N. Nitabach,
826 U. Heberlein, T. Preat, K. M. Branson, H. Tanimoto and G. M. Rubin (2014b). "Mushroom body
827 output neurons encode valence and guide memory-based action selection in Drosophila." *Elife* **3**:
828 e04580.

829 Baltruschat, L., L. Prisco, P. Ranft, J. S. Lauritzen, A. Fiala, D. D. Bock and G. Tavosanis (2021). "Circuit
830 reorganization in the Drosophila mushroom body calyx accompanies memory consolidation." *Cell*
831 *Rep* **34**(11): 108871.

832 Barth, M. and M. Heisenberg (1997). "Vision affects mushroom bodies and central complex in
833 Drosophila melanogaster." *Learn Mem* **4**(2): 219-229.

834 Barth, M., H. V. Hirsch, I. A. Meinertzhagen and M. Heisenberg (1997). "Experience-dependent
835 developmental plasticity in the optic lobe of Drosophila melanogaster." *J Neurosci* **17**(4): 1493-1504.

836 Berton, O., C. A. McClung, R. J. Dileone, V. Krishnan, W. Renthal, S. J. Russo, D. Graham, N. M.
837 Tsankova, C. A. Bolanos, M. Rios, L. M. Monteggia, D. W. Self and E. J. Nestler (2006). "Essential role
838 of BDNF in the mesolimbic dopamine pathway in social defeat stress." *Science* **311**(5762): 864-868.

839 Bharmauria, V., A. Ouelhazi, R. Lussiez and S. Molotchnikoff (2022). "Adaptation-induced plasticity
840 in the sensory cortex." *J Neurophysiol* **128**(4): 946-962.

841 Blochl, A. and C. Sirrenberg (1996). "Neurotrophins stimulate the release of dopamine from rat
842 mesencephalic neurons via Trk and p75Lntr receptors." *J Biol Chem* **271**(35): 21100-21107.

843 Bolus, H., K. Crocker, G. Boekhoff-Falk and S. Chtarbanova (2020). "Modeling Neurodegenerative
844 Disorders in Drosophila melanogaster." *Int J Mol Sci* **21**(9).

845 Boto, T., T. Louis, K. Jindachomthong, K. Jalink and S. M. Tomchik (2014). "Dopaminergic modulation
846 of cAMP drives nonlinear plasticity across the Drosophila mushroom body lobes." *Curr Biol* **24**(8):
847 822-831.

848 Boto, T., A. Stahl and S. M. Tomchik (2020). "Cellular and circuit mechanisms of olfactory associative
849 learning in Drosophila." *J Neurogenet* **34**(1): 36-46.

850 Bushey, D., G. Tononi and C. Cirelli (2011). "Sleep and synaptic homeostasis: structural evidence in
851 Drosophila." *Science* **332**(6037): 1576-1581.

852 Cachero, S., M. Gkantia, A. S. Bates, S. Frechter, L. Blackie, A. McCarthy, B. Sutcliffe, A. Strano, Y. Aso
853 and G. S. X. E. Jefferis (2020). "BAcTrace a new tool for retrograde tracing of neuronal circuit."
854 *Nature Methods* **17**: 1254-1261.

855 Carim-Todd, L., K. G. Bath, G. Fulgenzi, S. Yanpallewar, D. Jing, C. A. Barrick, J. Becker, H. Buckley, S.
856 G. Dorsey, F. S. Lee and L. Tessarollo (2009). "Endogenous truncated TrkB.T1 receptor regulates
857 neuronal complexity and TrkB kinase receptor function in vivo." *J Neurosci* **29**(3): 678-685.

858 Casarotto, P. C., M. Girych, S. M. Fred, V. Kovaleva, R. Moliner, G. Enkavi, C. Biojone, C. Cannarozzo,
859 M. P. Sahu, K. Kaurinkoski, C. A. Brunello, A. Steinzeig, F. Winkel, S. Patil, S. Vestring, T. Serchov, C.
860 Diniz, L. Laukkanen, I. Cardon, H. Antila, T. Rog, T. P. Piepponen, C. R. Bramham, C. Normann, S. E.
861 Lauri, M. Saarma, I. Vattulainen and E. Castren (2021). "Antidepressant drugs act by directly binding
862 to TRKB neurotrophin receptors." *Cell* **184**(5): 1299-1313 e1219.

863 Castren, E. and L. Monteggia (2021). "Brain-Derived Neurotrophic Factor Signaling in Depression
864 and Antidepressant Action." *Biol Psychiatry*.

865 Chan, R. F., G. Turecki, A. A. Shabalin, J. Guintivano, M. Zhao, L. Y. Xie, G. van Grootheest, Z. A.
866 Kaminsky, B. Dean, B. Penninx, K. A. Aberg and E. van den Oord (2020). "Cell Type-Specific
867 Methylome-wide Association Studies Implicate Neurotrophin and Innate Immune Signaling in Major
868 Depressive Disorder." *Biol Psychiatry* **87**(5): 431-442.

869 Chen, C. C. and J. C. Brumberg (2021). "Sensory Experience as a Regulator of Structural Plasticity in
870 the Developing Whisker-to-Barrel System." *Frontiers in Cellular Neuroscience* **15**.

871 Chen, C. C., J. K. Wu, H. W. Lin, T. P. Pai, T. F. Fu, C. L. Wu, T. Tully and A. S. Chiang (2012). "Visualizing
872 long-term memory formation in two neurons of the Drosophila brain." *Science* **335**(6069): 678-685.

873 Chen, C. Y., Y. C. Shih, Y. F. Hung and Y. P. Hsueh (2019). "Beyond defense: regulation of neuronal
874 morphogenesis and brain functions via Toll-like receptors." *J Biomed Sci* **26**(1): 90.

875 Cheng, L. K., Y. H. Chiu, Y. C. Lin, W. C. Li, T. Y. Hong, C. J. Yang, C. H. Shih, T. C. Yeh, W. I. Tseng, H.
876 Y. Yu, J. C. Hsieh and L. F. Chen (2022). "Long-term musical training induces white matter plasticity
877 in emotion and language networks." *Hum Brain Mapp*.

878 Coban, B., H. Poppinga, E. Y. Rachad, B. Geurten, D. Vasmer, F. J. Rodriguez Jimenez, Y. Gadgil, S. H.
879 Deimel, I. Alyagor, O. Schuldiner, I. C. Grunwald Kadow, T. D. Riemensperger, A. Widmann and A.
880 Fiala (2024). "The caloric value of food intake structurally adjusts a neuronal mushroom body circuit
881 mediating olfactory learning in Drosophila." *Learn Mem* **31**(5).

882 Costa, M., J. D. Manton, A. D. Ostrovsky, S. Prohaska and G. S. Jefferis (2016). "NBLAST: Rapid,
883 Sensitive Comparison of Neuronal Structure and Construction of Neuron Family Databases." *Neuron*
884 **91**(2): 293-311.

885 Cotman, C. W. and N. C. Berchtold (2002). "Exercise: a behavioral intervention to enhance brain
886 health and plasticity." *Trends Neurosci* **25**(6): 295-301.

887 Croset, V., C. D. Treiber and S. Waddell (2018). "Cellular diversity in the Drosophila midbrain
888 revealed by single-cell transcriptomics." *Elife* **7**.

889 DeLotto, Y. and R. DeLotto (1998). "Proteolytic processing of the Drosophila Spatzle protein by
890 easter generates a dimeric NGF-like molecule with ventralising activity." *Mech Dev* **72**(1-2): 141-
891 148.

892 Devaud, J. M., A. Acebes and A. Ferrus (2001). "Odor exposure causes central adaptation and
893 morphological changes in selected olfactory glomeruli in Drosophila." *J Neurosci* **21**(16): 6274-6282.

894 Duhart, J. M., A. Herrero, G. de la Cruz, J. I. Ispizua, N. Pirez and M. F. Ceriani (2020). "Circadian
895 Structural Plasticity Drives Remodeling of E Cell Output." *Curr Biol* **30**(24): 5040-5048 e5045.

896 Ernst, C., V. Deleva, X. Deng, A. Sequeira, A. Pomarenski, T. Klempan, N. Ernst, R. Quirion, A. Gratton,
897 M. Szyf and G. Turecki (2009). "Alternative splicing, methylation state, and expression profile of
898 tropomyosin-related kinase B in the frontal cortex of suicide completers." *Arch Gen Psychiatry* **66**(1):
899 22-32.

900 Eyjolfsdottir, E., S. Branson, X. P. Burgos-Artizzu, E. D. Hoopfer, J. Schor, D. J. Anderson and P. Perona
901 (2014). Detecting Social Actions of Fruit Flies, Cham, Springer International Publishing.

902 Feany, M. B. and W. W. Bender (2000). "A Drosophila model of Parkinson's disease." *Nature*
903 **404**(6776): 394-398.

904 Feldman, D. E. and M. Brecht (2005). "Map plasticity in somatosensory cortex." *Science* **310**(5749):
905 810-815.

906 Fenner, B. M. (2012). "Truncated TrkB: beyond a dominant negative receptor." *Cytokine Growth*
907 *Factor Rev* **23**(1-2): 15-24.

908 Fernandez, M. P., J. Berni and M. F. Ceriani (2008). "Circadian remodeling of neuronal circuits
909 involved in rhythmic behavior." *PLoS Biol* **6**(3): e69.

910 Ferrer, I., C. Marin, M. J. Rey, T. Ribalta, E. Goutan, R. Blanco, E. Tolosa and E. Marti (1999). "BDNF
911 and full-length and truncated TrkB expression in Alzheimer disease. Implications in therapeutic
912 strategies." *J Neuropathol Exp Neurol* **58**(7): 729-739.

913 Figueroa-Hall, L. K., M. P. Paulus and J. Savitz (2020). "Toll-Like Receptor Signaling in Depression."
914 *Psychoneuroendocrinology* **121**: 104843.

915 Foldi, I., N. Anthoney, N. Harrison, M. Gangloff, B. Verstak, M. P. Nallasivan, S. AlAhmed, B. Zhu, M.
916 Phizacklea, M. Losada-Perez, M. Moreira, N. J. Gay and A. Hidalgo (2017). "Three-tier regulation of
917 cell number plasticity by neurotrophins and Tolls in Drosophila." *J Cell Biol* **216**(5): 1421-1438.

918 Forero, M. G., K. Kato and A. Hidalgo (2012). "Automatic cell counting in vivo in the larval nervous
919 system of Drosophila." *J Microsc* **246**(2): 202-212.

920 Forero, M. G., A. R. Learte, S. Cartwright and A. Hidalgo (2010a). "DeadEasy Mito-Glia: automatic
921 counting of mitotic cells and glial cells in Drosophila." *PLoS One* **5**(5): e10557.

922 Forero, M. G., J. A. Pennack and A. Hidalgo (2010b). "DeadEasy neurons: automatic counting of HB9
923 neuronal nuclei in Drosophila." *Cytometry A* **77**(4): 371-378.

924 Forero, M. G., J. A. Pennack, A. R. Learte and A. Hidalgo (2009). "DeadEasy caspase: automatic
925 counting of apoptotic cells in Drosophila." *PLoS One* **4**(5): e5441.

926 Forrest, M. P., E. Parnell and P. Penzes (2018). "Dendritic structural plasticity and neuropsychiatric
927 disease." *Nat Rev Neurosci* **19**(4): 215-234.

928 Fryer, R. H., D. R. Kaplan, S. C. Feinstein, M. J. Radeke, D. R. Grayson and L. F. Kromer (1996).
929 "Developmental and mature expression of full-length and truncated TrkB receptors in the rat
930 forebrain." *J Comp Neurol* **374**(1): 21-40.

931 Fuentes-Medel, Y., M. A. Logan, J. Ashley, B. Ataman, V. Budnik and M. R. Freeman (2009). "Glia and
932 muscle sculpt neuromuscular arbors by engulfing destabilized synaptic boutons and shed
933 presynaptic debris." *PLoS Biol* **7**(8): e1000184.

934 Gage, F. H. (2019). "Adult neurogenesis in mammals." *Science* **364**(6443): 827-828.

935 Garrett, M. E., X. J. Qin, D. Mehta, M. F. Dennis, C. E. Marx, G. A. Grant, V. A. M.-A. M. Workgroup,
936 P. Initiative, Injury, C. Traumatic Stress Clinical, P. G. Psychiatric Genomics Consortium, M. B. Stein,
937 N. A. Kimbrel, J. C. Beckham, M. A. Hauser and A. E. Ashley-Koch (2021). "Gene Expression Analysis
938 in Three Posttraumatic Stress Disorder Cohorts Implicates Inflammation and Innate Immunity
939 Pathways and Uncovers Shared Genetic Risk With Major Depressive Disorder." *Front Neurosci* **15**:
940 678548.

941 Gay, N. J. and M. Gangloff (2007). "Structure and function of Toll receptors and their ligands." *Annu*
942 *Rev Biochem* **76**: 141-165.

943 Gorska-Andrzejak, J., A. Keller, T. Raabe, L. Kilianek and E. Pyza (2005). "Structural daily rhythms in
944 GFP-labelled neurons in the visual system of Drosophila melanogaster." *Photochem Photobiol Sci*
945 **4**(9): 721-726.

946 Guillin, O., J. Diaz, P. Carroll, N. Griffon, J. C. Schwartz and P. Sokoloff (2001). "BDNF controls
947 dopamine D3 receptor expression and triggers behavioural sensitization." *Nature* **411**(6833): 86-89.

948 Guven-Ozkan, T. and R. L. Davis (2014). "Functional neuroanatomy of Drosophila olfactory memory
949 formation." *Learn Mem* **21**(10): 519-526.

950 Harrison, N. J., E. Connolly, A. Gascon Gubieda, Z. Yang, B. Altenhein, M. Losada Perez, M. Moreira,
951 J. Sun and A. Hidalgo (2021). "Regenerative neurogenic response from glia requires insulin-driven
952 neuron-glia communication." *Elife* **10**.

953 Hearn, M. G., Y. Ren, E. W. McBride, I. Reveillaud, M. Beinborn and A. S. Kopin (2002). "A Drosophila
954 dopamine 2-like receptor: Molecular characterization and identification of multiple alternatively
955 spliced variants." *Proc Natl Acad Sci U S A* **99**(22): 14554-14559.

956 Heisenberg, M. (2003). "Mushroom body memoir: from maps to models." *Nat Rev Neurosci* **4**(4):
957 266-275.

958 Heisenberg, M., M. Heusipp and C. Wanke (1995). "Structural plasticity in the Drosophila brain." *J*
959 *Neurosci* **15**(3 Pt 1): 1951-1960.

960 Hepburn, L., T. K. Prajsnar, C. Klapholz, P. Moreno, C. A. Loynes, N. V. Ogryzko, K. Brown, M.
961 Schiebler, K. Hegyi, R. Antrobus, K. L. Hammond, J. Connolly, B. Ochoa, C. Bryant, M. Otto, B.
962 Surewaard, S. L. Seneviratne, D. M. Grogono, J. Cachat, T. Ny, A. Kaser, M. E. Torok, S. J. Peacock, M.
963 Holden, T. Blundell, L. Wang, P. Ligoxygakis, L. Minichiello, C. G. Woods, S. J. Foster, S. A. Renshaw
964 and R. A. Floto (2014). "Innate immunity. A Spaetzle-like role for nerve growth factor beta in
965 vertebrate immunity to Staphylococcus aureus." *Science* **346**(6209): 641-646.

966 Hoffmann, A., A. Funkner, P. Neumann, S. Juhnke, M. Walther, A. Schierhorn, U. Weininger, J.
967 Balbach, G. Reuter and M. T. Stubbs (2008a). "Biophysical characterization of refolded Drosophila
968 Spatzle, a cystine knot protein, reveals distinct properties of three isoforms." *J Biol Chem* **283**(47):
969 32598-32609.

970 Hoffmann, A., P. Neumann, A. Schierhorn and M. T. Stubbs (2008b). "Crystallization of Spatzle, a
971 cystine-knot protein involved in embryonic development and innate immunity in Drosophila
972 melanogaster." *Acta Crystallogr Sect F Struct Biol Cryst Commun* **64**(Pt 8): 707-710.

973 Holtmaat, A. and K. Svoboda (2009). "Experience-dependent structural synaptic plasticity in the
974 mammalian brain." *Nat Rev Neurosci* **10**(9): 647-658.

975 Horch, H. W. and L. C. Katz (2002). "BDNF release from single cells elicits local dendritic growth in
976 nearby neurons." *Nat Neurosci* **5**(11): 1177-1184.

977 Hu, X., Y. Yagi, T. Tanji, S. Zhou and Y. T. Ip (2004). "Multimerization and interaction of Toll and
978 Spatzle in Drosophila." *Proc Natl Acad Sci U S A* **101**(25): 9369-9374.

979 Huang, C., J. Luo, S. J. Woo, L. A. Roitman, J. Li, V. A. Pieribone, M. Kannan, G. Vasan and M. J.
980 Schnitzer (2024). "Dopamine-mediated interactions between short- and long-term memory
981 dynamics." *Nature*.

982 Hyman, C., M. Hofer, Y. A. Barde, M. Juhasz, G. D. Yancopoulos, S. P. Squinto and R. M. Lindsay
983 (1991). "BDNF is a neurotrophic factor for dopaminergic neurons of the substantia nigra." *Nature*
984 **350**(6315): 230-232.

985 Jenks, K. R., K. Tsimring, J. P. K. Ip, J. C. Zepeda and M. Sur (2021). "Heterosynaptic Plasticity and the
986 Experience-Dependent Refinement of Developing Neuronal Circuits." *Front Neural Circuits* **15**:
987 803401.

988 Kato, K., M. G. Forero, J. C. Fenton and A. Hidalgo (2011). "The glial regenerative response to central
989 nervous system injury is enabled by pros-notch and pros-NFkappaB feedback." *PLoS Biol* **9**(8):
990 e1001133.

991 Krashes, M. J. and S. Waddell (2008). "Rapid consolidation to a radish and protein synthesis-
992 dependent long-term memory after single-session appetitive olfactory conditioning in Drosophila."
993 *J Neurosci* **28**(12): 3103-3113.

994 Krashes, M. J. and S. Waddell (2011). "Drosophila appetitive olfactory conditioning." *Cold Spring*
995 *Harb Protoc* **2011**(5): pdb prot5609.

996 Kremer, M. C., F. Christiansen, F. Leiss, M. Paehler, S. Knapek, T. F. Andlauer, F. Forstner, P.
997 Kloppenburg, S. J. Sigrist and G. Tavosanis (2010). "Structural long-term changes at mushroom body
998 input synapses." *Curr Biol* **20**(21): 1938-1944.

999 Krishnan, V. and E. J. Nestler (2008). "The molecular neurobiology of depression." *Nature* **455**(7215):
1000 894-902.

1001 Kuner, R. and H. Flor (2016). "Structural plasticity and reorganisation in chronic pain." *Nat Rev*
1002 *Neurosci* **18**(1): 20-30.

1003 Lee, J. L., B. J. Everitt and K. L. Thomas (2004). "Independent cellular processes for hippocampal
1004 memory consolidation and reconsolidation." *Science* **304**(5672): 839-843.

1005 Leemhuis, E., L. De Gennaro and A. M. Pazzaglia (2019). "Disconnected Body Representation:
1006 Neuroplasticity Following Spinal Cord Injury." *J Clin Med* **8**(12).

1007 Levi-Montalcini, R., S. D. Skaper, R. Dal Toso, L. Petrelli and A. Leon (1996). "Nerve growth factor:
1008 from neurotrophin to neurokine." *Trends Neurosci* **19**(11): 514-520.

1009 Lewis, M., C. J. Arnot, H. Beeston, A. McCoy, A. E. Ashcroft, N. J. Gay and M. Gangloff (2013).
1010 "Cytokine Spatzle binds to the Drosophila immunoreceptor Toll with a neurotrophin-like specificity
1011 and couples receptor activation." *Proc Natl Acad Sci U S A* **110**(51): 20461-20466.

1012 Li, G., M. G. Forero, J. S. Wentzell, I. Durmus, R. Wolf, N. C. Anthoney, M. Parker, R. Jiang, J.
1013 Hasenauer, N. J. Strausfeld, M. Heisenberg and A. Hidalgo (2020). "A Toll-receptor map underlies
1014 structural brain plasticity." *Elife* **9**.

1015 Li, G. and A. Hidalgo (2021). "The Toll Route to Structural Brain Plasticity." *Front Physiol* **12**: 679766.

1016 Linneweber, G. A., M. Andriatsilavo, S. B. Dutta, M. Bengochea, L. Hellbruegge, G. Liu, R. K. Ejsmont,
1017 A. D. Straw, M. Wernet, P. R. Hiesinger and B. A. Hassan (2020). "A neurodevelopmental origin of
1018 behavioral individuality in the Drosophila visual system." *Science* **367**(6482): 1112-1119.

1019 Liu, C., P. Y. Placais, N. Yamagata, B. D. Pfeiffer, Y. Aso, A. B. Friedrich, I. Siwanowicz, G. M. Rubin, T.
1020 Preat and H. Tanimoto (2012). "A subset of dopamine neurons signals reward for odour memory in
1021 Drosophila." *Nature* **488**(7412): 512-516.

1022 Losada-Perez, M., N. Harrison and A. Hidalgo (2016). "Molecular mechanism of central nervous
1023 system repair by the Drosophila NG2 homologue kon-tiki." *J Cell Biol* **214**(5): 587-601.

1024 Lu, B., G. Nagappan, X. Guan, P. J. Nathan and P. Wren (2013). "BDNF-based synaptic repair as a
1025 disease-modifying strategy for neurodegenerative diseases." *Nat Rev Neurosci* **14**(6): 401-416.

1026 Lu, B., P. T. Pang and N. H. Woo (2005). "The yin and yang of neurotrophin action." *Nat Rev Neurosci*
1027 **6**(8): 603-614.

1028 Ma, Y., J. Li, I. Chiu, Y. Wang, J. A. Sloane, J. Lu, B. Kosaras, R. L. Sidman, J. J. Volpe and T. Vartanian
1029 (2006). "Toll-like receptor 8 functions as a negative regulator of neurite outgrowth and inducer of
1030 neuronal apoptosis." *J Cell Biol* **175**(2): 209-215.

1031 MacLaren, C. M., T. A. Evans, D. Alvarado and J. B. Duffy (2004). "Comparative analysis of the Kekkon
1032 molecules, related members of the LIG superfamily." *Dev Genes Evol* **214**(7): 360-366.

1033 Maguire, E. A., D. G. Gadian, I. S. Johnsrude, C. D. Good, J. Ashburner, R. S. Frackowiak and C. D.
1034 Frith (2000). "Navigation-related structural change in the hippocampi of taxi drivers." *Proc Natl Acad*
1035 *Sci U S A* **97**(8): 4398-4403.

1036 Mandai, K., T. Guo, C. St Hillaire, J. S. Meabon, K. C. Kanning, M. Bothwell and D. D. Ginty (2009).
1037 "LIG family receptor tyrosine kinase-associated proteins modulate growth factor signals during
1038 neural development." *Neuron* **63**(5): 614-627.

1039 Martinowich, K., H. Manji and B. Lu (2007). "New insights into BDNF function in depression and
1040 anxiety." *Nat Neurosci* **10**(9): 1089-1093.

1041 Mayseless, O., D. S. Berns, X. M. Yu, T. Riemensperger, A. Fiala and O. Schuldiner (2018).
1042 "Developmental Coordination during Olfactory Circuit Remodeling in Drosophila." *Neuron* **99**(6):
1043 1204-1215 e1205.

1044 McIlroy, G., I. Foldi, J. Aurikko, J. S. Wentzell, M. A. Lim, J. C. Fenton, N. J. Gay and A. Hidalgo (2013).
1045 "Toll-6 and Toll-7 function as neurotrophin receptors in the Drosophila melanogaster CNS." *Nat*
1046 *Neurosci* **16**(9): 1248-1256.

1047 McLaughlin, C. N., I. V. Nechipurenko, N. Liu and H. T. Broihier (2016). "A Toll receptor-FoxO pathway
1048 represses Pavarotti/MKLP1 to promote microtubule dynamics in motoneurons." *J Cell Biol* **214**(4):
1049 459-474.

1050 McLaughlin, C. N., J. J. Perry-Richardson, J. C. Coutinho-Budd and H. T. Broihier (2019). "Dying
1051 Neurons Utilize Innate Immune Signaling to Prime Glia for Phagocytosis during Development." *Dev*
1052 *Cell* **48**(4): 506-522 e506.

1053 Mehta, D., J. Voisey, D. Bruenig, W. Harvey, C. P. Morris, B. Lawford and R. M. Young (2018).
1054 "Transcriptome analysis reveals novel genes and immune networks dysregulated in veterans with
1055 PTSD." *Brain Behav Immun* **74**: 133-142.

1056 Meyer, S. N., M. Amoyel, C. Bergantinos, C. de la Cova, C. Schertel, K. Basler and L. A. Johnston
1057 (2014). "An ancient defense system eliminates unfit cells from developing tissues during cell
1058 competition." *Science* **346**(6214): 1258236.

1059 Minichiello, L. (2009). "TrkB signalling pathways in LTP and learning." *Nat Rev Neurosci* **10**(12): 850-
1060 860.

1061 Nern, A., B. D. Pfeiffer and G. M. Rubin (2015). "Optimized tools for multicolor stochastic labeling
1062 reveal diverse stereotyped cell arrangements in the fly visual system." *Proc Natl Acad Sci U S A*
1063 **112**(22): E2967-2976.

1064 Neve, K. A., J. K. Seamans and H. Trantham-Davidson (2004). "Dopamine receptor signaling." *J*
1065 *Recept Signal Transduct Res* **24**(3): 165-205.

1066 Ohira, K. and M. Hayashi (2009). "A new aspect of the TrkB signaling pathway in neural plasticity."
1067 *Curr Neuropharmacol* **7**(4): 276-285.

1068 Ohira, K., K. J. Homma, H. Hirai, S. Nakamura and M. Hayashi (2006). "TrkB-T1 regulates the RhoA
1069 signaling and actin cytoskeleton in glioma cells." *Biochem Biophys Res Commun* **342**(3): 867-874.

1070 Okun, E., K. Griffioen, B. Barak, N. J. Roberts, K. Castro, M. A. Pita, A. Cheng, M. R. Mughal, R. Wan,
1071 U. Ashery and M. P. Mattson (2010). "Toll-like receptor 3 inhibits memory retention and constrains
1072 adult hippocampal neurogenesis." *Proc Natl Acad Sci U S A* **107**(35): 15625-15630.

1073 Okun, E., K. J. Griffioen and M. P. Mattson (2011). "Toll-like receptor signaling in neural plasticity
1074 and disease." *Trends Neurosci* **34**(5): 269-281.

1075 Pare, A. C., A. Vichas, C. T. Fincher, Z. Mirman, D. L. Farrell, A. Mainieri and J. A. Zallen (2014). "A
1076 positional Toll receptor code directs convergent extension in Drosophila." *Nature* **515**(7528): 523-
1077 527.

1078 Park, H. and M. M. Poo (2013). "Neurotrophin regulation of neural circuit development and
1079 function." *Nat Rev Neurosci* **14**(1): 7-23.

1080 Patel, V., A. M. Patel and J. J. McArdle (2016). "Synaptic abnormalities of mice lacking toll-like
1081 receptor (TLR)-9." *Neuroscience* **324**: 1-10.

1082 Pech, U., N. H. Revelo, K. J. Seitz, S. O. Rizzoli and A. Fiala (2015). "Optical dissection of experience-
1083 dependent pre- and postsynaptic plasticity in the Drosophila brain." *Cell Rep* **10**(12): 2083-2095.

1084 Placais, P. Y., E. de Tredern, L. Scheunemann, S. Trannoy, V. Goguel, K. A. Han, G. Isabel and T. Preat
1085 (2017). "Upregulated energy metabolism in the Drosophila mushroom body is the trigger for long-
1086 term memory." *Nat Commun* **8**: 15510.

1087 Placais, P. Y., S. Trannoy, G. Isabel, Y. Aso, I. Siwanowicz, G. Belliart-Guerin, P. Vernier, S. Birman, H.
1088 Tanimoto and T. Preat (2012). "Slow oscillations in two pairs of dopaminergic neurons gate long-
1089 term memory formation in Drosophila." *Nat Neurosci* **15**(4): 592-599.

1090 Poo, M. M. (2001). "Neurotrophins as synaptic modulators." *Nat Rev Neurosci* **2**(1): 24-32.

1091 Riemensperger, T., G. Isabel, H. Coulom, K. Neuser, L. Seugnet, K. Kume, M. Iche-Torres, M. Cassar,
1092 R. Strauss, T. Preat, J. Hirsh and S. Birman (2011). "Behavioral consequences of dopamine deficiency
1093 in the Drosophila central nervous system." *Proc Natl Acad Sci U S A* **108**(2): 834-839.

1094 Riemensperger, T., A. R. Issa, U. Pech, H. Coulom, M. V. Nguyen, M. Cassar, M. Jacquet, A. Fiala and
1095 S. Birman (2013). "A single dopamine pathway underlies progressive locomotor deficits in a
1096 Drosophila model of Parkinson disease." *Cell Rep* **5**(4): 952-960.

1097 Rolls, A., R. Shechter, A. London, Y. Ziv, A. Ronen, R. Levy and M. Schwartz (2007). "Toll-like receptors
1098 modulate adult hippocampal neurogenesis." *Nat Cell Biol* **9**(9): 1081-1088.

1099 Sachse, S., E. Rueckert, A. Keller, R. Okada, N. K. Tanaka, K. Ito and L. B. Vosshall (2007). "Activity-
1100 dependent plasticity in an olfactory circuit." *Neuron* **56**(5): 838-850.

1101 Sahu, M. P., Y. Pazos-Boubeta, C. Pajanoja, S. Rozov, P. Panula and E. Castren (2019). "Neurotrophin
1102 receptor Ntrk2b function in the maintenance of dopamine and serotonin neurons in zebrafish." *Sci*
1103 *Rep* **9**(1): 2036.

1104 Shafer, O. T., D. J. Kim, R. Dunbar-Yaffe, V. O. Nikolaev, M. J. Lohse and P. H. Taghert (2008).
1105 "Widespread receptivity to neuropeptide PDF throughout the neuronal circadian clock network of
1106 Drosophila revealed by real-time cyclic AMP imaging." *Neuron* **58**(2): 223-237.

1107 Sharma, A. (2012). "Genome-wide expression analysis in epilepsy: a synthetic review." *Curr Top Med*
1108 *Chem* **12**(9): 1008-1032.

1109 Squillace, S. and D. Salvemini (2022). "Toll-like receptor-mediated neuroinflammation: relevance for
1110 cognitive dysfunctions." *Trends Pharmacol Sci* **43**(9): 726-739.

1111 Stoilov, P., E. Castren and S. Stamm (2002). "Analysis of the human TrkB gene genomic organization
1112 reveals novel TrkB isoforms, unusual gene length, and splicing mechanism." *Biochem Biophys Res*
1113 *Commun* **290**(3): 1054-1065.

1114 Sugie, A., S. Hakeda-Suzuki, E. Suzuki, M. Silies, M. Shimozono, C. Mohl, T. Suzuki and G. Tavosanis
1115 (2015). "Molecular Remodeling of the Presynaptic Active Zone of Drosophila Photoreceptors via
1116 Activity-Dependent Feedback." *Neuron* **86**(3): 711-725.

1117 Sun, J., A. Q. Xu, J. Giraud, H. Poppinga, T. Riemensperger, A. Fiala and S. Birman (2018). "Neural
1118 Control of Startle-Induced Locomotion by the Mushroom Bodies and Associated Neurons in
1119 Drosophila." *Front Syst Neurosci* **12**: 6.

1120 Sur, M. and J. L. Rubenstein (2005). "Patterning and plasticity of the cerebral cortex." *Science*
1121 **310**(5749): 805-810.

1122 Sutcliffe, B., M. G. Forero, B. Zhu, I. M. Robinson and A. Hidalgo (2013). "Neuron-type specific
1123 functions of DNT1, DNT2 and Spz at the Drosophila neuromuscular junction." *PLoS One* **8**(10):
1124 e75902.

1125 Talay, M., E. B. Richman, N. J. Snell, G. G. Hartmann, J. D. Fisher, A. Sorkac, J. F. Santoyo, C. Chou-
1126 Freed, N. Nair, M. Johnson, J. R. Szymanski and G. Barnea (2017). "Transsynaptic Mapping of Second-
1127 Order Taste Neurons in Flies by trans-Tango." *Neuron* **96**(4): 783-795 e784.

1128 Tamada, M., J. Shi, K. S. Bourdot, S. Supriyatno, K. H. Palmquist, O. L. Gutierrez-Ruiz and J. A. Zallen
1129 (2021). "Toll receptors remodel epithelia by directing planar-polarized Src and PI3K activity." *Dev*
1130 *Cell* **56**(11): 1589-1602 e1589.

1131 Tauszig, S., E. Jouanguy, J. A. Hoffmann and J. L. Imler (2000). "Toll-related receptors and the control
1132 of antimicrobial peptide expression in Drosophila." *Proc Natl Acad Sci U S A* **97**(19): 10520-10525.

1133 Technau, G. M. (1984). "Fiber number in the mushroom bodies of adult Drosophila melanogaster
1134 depends on age, sex and experience." *J Neurogenet* **1**(2): 113-126.

1135 Tempel, B. L., N. Bonini, D. R. Dawson and W. G. Quinn (1983). "Reward learning in normal and
1136 mutant Drosophila." *Proc Natl Acad Sci U S A* **80**(5): 1482-1486.

1137 Tessarollo, L. and S. Yanpallewar (2022). "TrkB Truncated Isoform Receptors as Transducers and
1138 Determinants of BDNF Functions." *Front Neurosci* **16**: 847572.

1139 Ulian-Benitez, S., S. Bishop, I. Foldi, J. Wentzell, C. Okenwa, M. G. Forero, B. Zhu, M. Moreira, M.
1140 Phizacklea, G. McIlroy, G. Li, N. J. Gay and A. Hidalgo (2017). "Kek-6: A truncated-Trk-like receptor
1141 for Drosophila neurotrophin 2 regulates structural synaptic plasticity." *PLoS Genet* **13**(8): e1006968.

1142 Vahid-Ansari, F. and P. R. Albert (2021). "Rewiring of the Serotonin System in Major Depression."
1143 *Front Psychiatry* **12**: 802581.

1144 Vaughen, J. P., E. Theisen, I. M. Rivas-Serna, A. B. Berger, P. Kalakuntla, I. Anreiter, V. C. Mazurak, T.
1145 P. Rodriguez, J. D. Mast, T. Hartl, E. O. Perlstein, R. J. Reimer, M. T. Clandinin and T. R. Clandinin
1146 (2022). "Glial control of sphingolipid levels sculpts diurnal remodeling in a circadian circuit." *Neuron*
1147 **110**(19): 3186-3205 e3187.

1148 Waddell, S. (2013). "Reinforcement signalling in Drosophila; dopamine does it all after all." *Curr Opin*
1149 *Neurobiol* **23**(3): 324-329.

1150 Wang, C. S., E. T. Kavalali and L. M. Monteggia (2022). "BDNF signaling in context: From synaptic
1151 regulation to psychiatric disorders." *Cell* **185**(1): 62-76.

1152 Ward, A., W. Hong, V. Favaloro and L. Luo (2015). "Toll receptors instruct axon and dendrite
1153 targeting and participate in synaptic partner matching in a Drosophila olfactory circuit." *Neuron*
1154 **85**(5): 1013-1028.

1155 Weber, A. N., S. Tauszig-Delamasure, J. A. Hoffmann, E. Lelievre, H. Gascan, K. P. Ray, M. A. Morse,
1156 J. L. Imler and N. J. Gay (2003). "Binding of the Drosophila cytokine Spatzle to Toll is direct and
1157 establishes signaling." *Nat Immunol* **4**(8): 794-800.

1158 Wiesel, T. N. (1982). "Postnatal development of the visual cortex and the influence of environment."
1159 *Nature* **299**(5884): 583-591.

1160 Wohleb, E. S., T. Franklin, M. Iwata and R. S. Duman (2016). "Integrating neuroimmune systems in
1161 the neurobiology of depression." *Nat Rev Neurosci* **17**(8): 497-511.

1162 Woollett, K. and E. A. Maguire (2011). "Acquiring "the Knowledge" of London's layout drives
1163 structural brain changes." *Curr Biol* **21**(24): 2109-2114.

1164 Yacoubian, T. A. and D. C. Lo (2000). "Truncated and full-length TrkB receptors regulate distinct
1165 modes of dendritic growth." *Nat Neurosci* **3**(4): 342-349.

1166 Yang, T., Z. Nie, H. Shu, Y. Kuang, X. Chen, J. Cheng, S. Yu and H. Liu (2020). "The Role of BDNF on
1167 Neural Plasticity in Depression." *Front Cell Neurosci* **14**: 82.

1168 Zhang, J., T. Tang, R. Zhang, L. Wen, X. Deng, X. Xu, W. Yang, F. Jin, Y. Cao, Y. Lu and X. Q. Yu (2024).
1169 "Maintaining Toll signaling in Drosophila brain is required to sustain autophagy for dopamine
1170 neuron survival." *iScience* **27**(2): 108795.

1171 Zhu, B., J. A. Pennack, P. McQuilton, M. G. Forero, K. Mizuguchi, B. Sutcliffe, C. J. Gu, J. C. Fenton
1172 and A. Hidalgo (2008). "Drosophila neurotrophins reveal a common mechanism for nervous system
1173 formation." *PLoS Biol* **6**(11): e284.
1174

1175

1176 FIGURE LEGENDS

1177 **Figure 1 Neurons expressing *DNT-2* and its receptors *Toll-6* and *kek-6* in the adult brain**

1178 **(A, B)** *DNT-2A* expressing neurons (*DNT-2>FlyBow1.1* in green; anti-Brp in magenta) have cell bodies in SOG
1179 and project to FLA/PRW and SMP. **(C, C', C'')** Pre-synaptic (green) and post-synaptic (magenta) terminals of
1180 DNT-2A neurons seen with *DNT-2>DenMark::RFP, Dsyd1::GFP*, higher magnification in **(C',C''),** different
1181 specimens from (C). DNT-2A projections at SMP and PRW have both pre- and post-synaptic sites. **(D)** Single
1182 neuron DNT-2A>MCFO clones. **(E)** DNT-2A neurons have the vesicular glutamate transporter vGlut
1183 (arrows). **(F)** Colocalization between *Dop2RLex>AopCD8-GFP* and *DNT2Gal4>UASCD8-RFP* in cell bodies of
1184 DNT-2A neurons (arrows). **(G)** Terminals of dopaminergic neurons (*TH>mCD8GFP*) abut and overlap those
1185 of DNT-2A neurons (*DNT2>CD8-RFP*, magenta), arrows; magnified projections on the right. **(H)** Illustration
1186 of neurons expressing DNT-2 (magenta) and KCs, DAN PAM and PPL1, and DAL neurons **(I)** *Toll-6>FlyBow1.1*
1187 is expressed in Kenyon cells, PPL1, PPL2 and PAM DANs, as revealed by co-localization with anti-TH. **(J)** *kek-*
1188 *6>FlyBow1.1* co-localises with TH in MB vertical lobes, dopaminergic PALs, VUMs, PPL1, PPM2 and PPM3.

1189 SMP: superior medial protocerebrum, PRW: Prow, FLA: Flange, SOG: sub-aesophageal ganglion. Scale bars:
1190 (A, H, I) 50µm; (B,C,C", D,G) 30µm (C', F,) 25µm.
1191
1192 **Figure 2 DNT-2 neurons are functionally connected to dopaminergic neurons**
1193 **(A)** TransTango revealed out-puts of DNT-2 neurons. All neurons express *TransTango* and expression of the
1194 TransTango ligand in DNT-2 neurons identified DNT-2 out-puts with Tomato (anti-DsRed). TransTango
1195 identified as DNT-2 outputs KC $\alpha'\beta'$ MB lobes (anterior brain, arrow, **top left**); Kenyon and possibly DAN cell
1196 bodies (posterior, arrows **top right**); DAL neurons **(bottom left,** arrows) and the dorsal layer of the fan
1197 shaped body **(bottom right,** arrow). See also Supplementary Figure S3 for further controls. **(B)** BAcTrace
1198 tests connectivity to a candidate neuron input visualised with *LexAop>sybGFP* by driving the expression of a
1199 ligand from *DNT-2GAL4* that will activate *QUASTomato* in the candidate input neuron (Cachero et al. 2020).
1200 Candidate PAM neurons visualised at SMP with GFP (green): Control: *R58E02LexA>BAcTrace 806*, no *GAL4*.
1201 Test: *R58E02LexA, DNT-2GAL4>BAcTrace 806* revealed PAMs are inputs of DNT-2A neurons at SMP
1202 (Tomato, bottom). Magenta shows QUAS-Tomato. **(C)** qRT-PCR showing that TH mRNA levels increased
1203 with DNT-2 over-expression at 30°C *(tubGAL80^{ts}, DNT-2>DNT-2FL).* One way ANOVA, P=0.0085; post-doc
1204 Dunnett's multiple comparison test**. (D)** FRET cAMP probe Epac1 revealed that *DNT-2>Dop2R-RNAi*
1205 knockdown decreased YFP/CFP ratio over time in DNT-2A neurons, meaning that cAMP levels increased.
1206 Two-way ANOVA, genotype factor p<0.0001, time factor p<0.0001; post-doc Dunnett's. **(E,F)** Summary:
1207 DNT-2 neurons and DANs are functionally connected and modulate each other. **(E)** DNT-2 can induce *TH*
1208 expression in DANs; **(F)** this is followed by negative feedback from DANs to DNT-2 neurons (question marks
1209 indicate inferences). TH: tyrosine hydroxylase. Scale bars: (A) 50µm; (B) 30µm; (D) 20µm. P values over
1210 graphs in (C) refer to group analyses; stars indicate multiple comparisons tests. *p<0.05,**p<0.01,
1211 ***p<0.001. For sample sizes and further statistical details, see Supplementary Table S2.
1212
1213 **Figure 3 DNT-2 and Toll-6 maintain PAM neuron survival in the developing and adult brain.**

1214 **(A)** Illustration of PAM neuronal cell bodies and experimental temporal profile. DANs are shown in green,
1215 DNT-2A neurons in magenta and MB in dark grey. The left hemisphere shows the anterior brain with PAL
1216 and PAM DAN neurons (green) and DNT-2 neurons (magenta); the right shows the posterior brain, with the
1217 calyx and other DAN neurons (PPM1, PPM2, PPM3, PPL1, PPL2, green). **(B-D)** Fruit-flies were kept
1218 constantly at 25°C, from development to adult. Analyses done in adult brains**. (B)** *DNT-2^{37}/DNT-2^{18}* mutants
1219 had fewer histone-YFP+ labelled PAM neurons (*THGAL4, R58E02-GAL4>hisYFP).* Un-paired Student t-test.
1220 **(C)** *Toll-6* RNAi knock-down in all DANs (*THGAL4, R58E02-GAL4>hisYFP, Toll-6 RNAi)* reduced Histone-YFP+
1221 labelled PAM cell number. Un-paired Student t-test. **(D)** *DNT-2^{37}/DNT-2^{18}* mutants had fewer PAMs stained
1222 with anti-TH antibodies. Over-expressing *Toll-6^{CY}* in DANs (*THGAL4, R58E02 GAL4>hisYFP, Toll-6^{CY}*) rescued
1223 TH+ PAM neurons in *DNT-2^{37}/DNT-2^{18}* mutants, demonstrating that DNT-2 functions via Toll-6 to maintain
1224 PAM cell survival. Welch ANOVA p<0.0001, post-hoc Dunnett test. **(E-H)** Adult specific restricted over-
1225 expression or knock-down at 30°C, using the temperature sensitive GAL4 repressor *tubGAL80^{ts}*. **(E)** Adult
1226 specific *DNT-2* RNAi knockdown in DNT-2 neurons decreased Tomato+ PAM cell number (*tubGAL80^{ts},*
1227 *R58E02-LexA, DNT-2 GAL4>LexAOP-Tomato, UAS DNT-2-RNAi*). Un-paired Student t-test, p= 0.005. **(F)** Adult
1228 specific *Toll-6* RNAi knock-down in *Toll-6^{31}* heterozygous mutant flies in DANs, reduced Histone-YFP+ PAM
1229 cell number (*tubGAL80^{ts}; THGAL4, R58E02-GAL4>hisYFP, Toll-6 RNAi/Toll6^{31}*). Un-paired Student t-test. **(G)**
1230 PAMs were visualised with anti-TH. Left: *tubGAL80^{ts}, Toll-6>Toll-6-RNAi* knock-down decreased TH+ PAM
1231 cell number. Un-paired Student t-test. Right: *tubGAL80^{ts}, DNT-2>DNT-2-RNAi* knock-down decreased TH+
1232 PAM cell number, whereas *DNT-2FL* over-expression increased PAM cell number. Kruskal-Wallis ANOVA,
1233 p=0.0001, post-hoc Dunn's test. **(H)** Adult-specific *tubGAL80^{ts}, DNT-2>DNT-2RNAi* knock-down increased
1234 the number of apoptotic cells in the brain labelled with anti-DCP-1. Dcp-1+ cells co-localise with anti-TH at
1235 least in PAM clusters. One Way ANOVA, p<0.0001, post-doc Bonferroni's multiple comparisons test.
1236 DANs>histone-YFP: all dopaminergic neurons expressing histone-YFP, genotype: *THGal4 R58E02Gal4>UAS-*
1237 *histoneYFP*. *PAMsLexA>tomato*: restricted to PAM DANs: *R58E02LexA>LexAop-nlstdTomato.* Controls: *GAL4*
1238 drivers crossed to wild-type Canton-S. Scale bars: (B-G) 30µm; (H) 20µm. Graphs show box-plots around the
1239 median. P values over graphs in (D, G right, H) refer to group analyses; stars indicate multiple comparisons

1240 tests. *p<0.05, **p<0.01, ***p<0.001. For further genotypes, sample sizes and statistical details, see
1241 Supplementary Table S2.
1242
1243 **Figure 4 DNT-2, Toll-6 and Kek-6 are required for arborisations and synapse formation. (A)**
1244 Illustration showing the ROIs (dashed lines) used for the analyses, corresponding to dendrites and axonal
1245 endings of PAMs and axonal terminals of PPL1ped neurons. **(B-F)** Fruit-flies were kept constantly at 25°C.
1246 **(B)** Complete loss of DAN synapses *(TH, R58E02>sytGFP)* onto α,β MB lobe in *DNT-2* null mutants. **(C)** *Toll-6*
1247 RNAi knockdown in PAM β2β'2 neurons (*MB301B>FB1.1, Toll-6-RNAi*) decreased dendrite complexity. Un-
1248 paired Student t-test. **(D)** Over-expression of cleaved *DNT-2CK* in PAM β2β'2 neurons *(MB301B>CD8-GFP,*
1249 *DNT-2CK)* increased dendrite complexity. Un-paired Student t-test. **(E,E',F)** PPL1ped axonal misrouting was
1250 visualised with *split-GAL4 MB320CGal4>FlyBow1.1.* Images show PPL1-γped neurons and some PPL1-
1251 α2α'2. **(D,D')** RNAi knock-down of *Toll-6, kek-6* or both (e.g. *MB320CGal4>FlyBow1.1, Toll-6RNAi)* in PPL1-
1252 γped neurons caused axonal terminal misrouting (arrows). **(E')** Higher magnification of **(E,** dotted squares**)**.
1253 Chi-square for group analysis: p = 0.0224, and multiple comparisons Bonferroni correction control vs *Toll-*
1254 *6RNAi* p<0.01; vs *kek-6RNAi* p<0.05; vs *Toll-6RNAi kek-6RNAi* p<0.01, see Table S2**. (F)** PPL1 misrouting was
1255 also induced by over-expressed *DNT-2CK* or *DNT-2FL* (e.g. *MB320CGal4>FlyBow1.1, DNT-2FL)*. Chi-square
1256 for group analysis: p<0.05, Bonferroni correction control vs *DNT-2CK* ns, vs *DNT-2FL* *p<0.05, see Table S2.
1257 **(G)** Adult-specific *Toll-6 kek-6 RNAi* knockdown in PAM neurons decreased size of post-synaptic density
1258 sites (*PAM>Homer-GCaMP* and anti-GFP antibodies). Temperature regime shown on the right. **(C,D)** Graphs
1259 show box-plots around the median; **(G)** are box-plots with dot plots. (C,D,G) *p<0.05, **p<0.01,
1260 ****p<0.0001. Scale bars: (B,C,D,E) 30µm; (E',F,G) 20µm. For genotypes, sample sizes and statistical details,
1261 see Supplementary Table S2.
1262
1263 **Figure 5 DNT-2 neuron activation and DNT-2 over-expression induced synaptogenesis. (A)**
1264 Thermo-activation of DNT-2 neurons at 30°C altered DNT-2 arborisations, here showing an example with
1265 smaller dendrites and enlarged axonal arbours (magenta shows 3D-rendering of axonal arborisation done

1266 with Imaris, merged with raw image in green). (Genotype: *DNT-2>FlyBow1.1, TrpA1*). **(B)** Thermogenetic
1267 activation of DNT-2 neurons increased the number of Homer+ PSDs in DNT-2 neurons, at SMP (*DNT-*
1268 *2>Homer-GCAMP3, TrpA1*, anti-GFP). Test at 30°C 24h: Unpaired Student t test. See Table S2. **(C)**
1269 Thermogenetic activation of DNT-2 neurons induced synaptogenesis in PAM target neurons at SMP, but not
1270 at MB lobe. (Genotype: *PAM(R58E02)LexA/LexAOP-sytGCaMP; DNT-2GAL4/UASTrpA1*). At SMP: No. Syt+
1271 synapses: Mann Whitney-U; Syt+ synapse volume: Mann Whitney-U. At MB lobe: No. Syt+ synapses:
1272 Unpaired Student t ns; Syt+ synapse volume: Mann Whitney-U ns. **(D)** Over-expression of *DNT-2FL* in DNT-
1273 2 neurons increased synapse volume at SMP dendrite and induced synaptogenesis at MB lobe. (Genotype:
1274 *PAM(R58E02)LexA/LexAopSytGcaMP6; DNT-2Gal4/UAS-DNT-2FL*). At SMP: No. Syt+ synapses: Unpaired
1275 Student t ns. Syt+ synapse volume: Mann Whitney-U. At MB lobe: No. Syt+ synapses: Unpaired Student t;
1276 Syt+ synapse volume: Mann Whitney-U ns. Graphs show box-plots around the median, except for PSD
1277 volume data that are dot plots. *p<0.05, ****p<0.0001; ns: not significantly different from control. Scale
1278 bars: 30µm. For Genotypes, sample sizes, p values and other statistical details, see Supplementary Table S2.
1279

1280 **Figure 6 DNT-2-induced circuit plasticity modified dopamine-dependent behaviour. (A)** *DNT-2*
1281 mutants (left, *DNT-2^{37}/DNT-2^{18}*) and flies with adult-specific RNAi knock-down of *DNT-2* in DNT-2 neurons
1282 (right, *tubGAL80^{ts}; DNT-2>DNT-2RNAi*), had impaired climbing. Left Mann Whitney U; Right: One Way
1283 ANOV, post-hoc Dunnett. **(B)** Adult-specific *Toll-6* and *kek-6* RNAi knock-down in Toll-6 *(tubGAL80^{ts}; Toll-*
1284 *6>Toll-6RNAi, kek-6RNAi,* left) or PAM (*tubGAL80^{ts}; R58E02>Toll-6RNAi, kek-6RNAi,* right) neurons impaired
1285 climbing. Left: Welch ANOVA, post-hoc Dunnett. Right: Welch ANOVA, post-hoc Dunnett. **(C)** The climbing
1286 impairment of *DNT-2* mutants could be rescued with the over-expression of *Toll-6^{CY}* in dopaminergic
1287 neurons (Rescue genotype: UASToll-6^{CY}/+; DNT-2^{18}*THGAL4 R58E02GAL4/DNT-2^{37}).* Welch ANOVA, post-hoc
1288 Dunnett. **(D)** Adult specific over-expression of *Toll-6^{CY}* in DANs increased locomotion in *DNT-2^{37}/DNT-2^{18}*
1289 mutants. (Test genotype: *UASToll-6^{CY}/+; DNT-2^{18}THGAL4 R58E02GAL4/DNT-2^{37}*). Walking speed: Kruskal
1290 Wallis ANOVA, post-hoc Dunn's. Distance walked: Kruskal Wallis ANOVA, post-hoc Dunn's. Time spent
1291 immobile: Kruskal Wallis ANOVA, post-hoc Dunn's. **(E)** Adult specific *DNT-2FL* overexpression in DNT-2

1292 neurons increased fruit-fly locomotion speed in an open arena at 30°C (see also Supplementary Figure S6A
1293 for further controls). (Test genotype: *tubGAL80^{ts}, DNT-2>DNT-2FL*) Kruskal-Wallis, post-hoc Dunn's test. **(F)**
1294 Thermogenetic activation of DNT-2 neurons at 30°C *(DNT-2>TrpA1)* increased fruit-fly locomotion speed.
1295 (See also Supplementary Figure S6B for further controls). One Way ANOVA p<0.0001, post-hoc Dunnett's
1296 test**. (G)** Over-expression of *DNT-2-FL* in DNT-2 neurons increased long-term memory. (Test genotype:
1297 *tubGAL80^{ts}, DNT-2>DNT-2FL*). Left: 23°C controls: One Way ANOVA p=0.8006. Right 30°C: One Way ANOVA,
1298 post-hoc Dunnett's test. Graphs show box-plots around the median, under also dot plots. P values over
1299 graphs refer to group analyses; asterisks indicate multiple comparisons tests. *p<0.05, **p<0.01,
1300 ***p<0.001, ****p<0.0001; ns: not significantly different from control. For further genotypes, sample sizes,
1301 p values and other statistical details, see Supplementary Table S2.
1302
1303 SUPPLEMENTAL INFORMATION
1304 **Supplementary Figure S1 Identification of neurotransmitter type for DNT-2A neurons. (A)** All four
1305 DNT-2A neurons per hemibrain are glutamatergic as DNT-2>FlyBow1.1 reporter co-localises with anti-vGlut
1306 in these neurons as well as in their projections at SMP (arrows point at cluster of 4 cells). **(B)** All four DNT-
1307 2A neurons per hemibrain have Dop2R (arrows point to cluster, each neuron seen in magenta). **(C, D)**
1308 Anterior DNT-2A neurons projecting at SMP are not dopaminergic, as there was no co-localisation between
1309 *DNT-2>histoneYFP* and anti-TH in the anterior brain **(C),** and there was no colocalization in other DNT-2+
1310 neurons in the posterior brain either **(D).** Higher magnification of dotted boxes on the right. **(E)** There was
1311 no colocalisation with *Dop1R2LexA>CD8::GFP, DNT-2Gal4>CD8::RFP* either. **(F)** DNT-2 neurons are not
1312 serotonergic, as there was no co-localization between *DNT-2>FlyBow1.1* and the serotoninergic neuron
1313 marker anti-5HT**. (G)** They are not octopaminergic, as there was no overlap between *TdcLexA>mCD8::GFP*
1314 *and DNT-2Gal4>CD8::RFP*. **(H)** There was no overlap between *DNT-2Gal4>histoneYFP* and the cholinergic
1315 neuron marker anti-ChAT4b1. **(I,J)** Anterior DNT-2A neurons are not GABAergic, but lateral DNT-2 neurons
1316 are, as visualised with *DNT-2>CD8-RFP, GADLexA>CD8-GFP*. Scale bars: (A right,B, F, G, H, I, J) 20µm; (C,D)
1317 50 µm. For further genotypes and sample sizes, see Supplementary Table S2.

1318

1319 **Supplementary Figure S2 Identification of *Toll-6* and *kek-6* expressing neurons. (A)** *Toll-6Gal4,*
1320 *MB247-Gal80>UASFlyBow1.1* and *kek-6Gal4, MB247-Gal80>UASFlyBow1.1* revealed Toll-6+ and Kek-6+
1321 projections on MB g2a'1. **(B)** *R25D01LexA>CD8GFP, kek6-Gal4>CD8RFP* overlapped in MB g2a'1. **(C)**
1322 *R14C08LexA>CD8GFP, Toll-6Gal4>CD8-RFP13* revealed co-localization in MBON-M4/M6 cell bodies. **(D,E)**
1323 Co-localisation of *Toll-6>Histone-YFP* and *kek-6>HistoneYFP* with TH in PPL1 neurons. **(F)** Number of PAM
1324 and PPL1 neurons expressing *Tolls* and *kek-6,* revealed from published RNAseq data (Scope, see also Table
1325 S1). **(G, H)** Toll-6 and kek-6 are expressed in DAL neurons. **(G)** DAL neurons express *Toll-6,* as revealed by
1326 co-localization between *DAL-LexA (VT49239-LexA)>mCD8-GFP* and *Toll-6GAL4>mCD8-RFP*. **(H)** DAL neurons
1327 express *kek-6*, as revealed by colocalization between *DAL-LexA (VT49239-LexA)>mCD8-GFP* and
1328 *kek6GAL4>mCD8RFP*. **(I, J)** Toll-6 and kek-6 are expressed in MB neurons. **(I)** *Toll-6>MCFO* clones reveal
1329 expression at least in MB neurons g medial (gm), abcore (abc) and absurface (abs). **(K)** *kek-6>MCFO* clones
1330 reveal expression at least in MB Kenyon cells aba'b'g formed and MB g2a'1 and a2a'2 and PPL1-γ2α'1 and
1331 PPL1-α2α'2. Scale bars: (B, H) 50µm; (A,C,D,G, I, J) 30µm. For further genotypes and sample sizes, see
1332 Supplementary Table S2.

1333

1334 **Supplementary Figure S3 TransTango connectivity controls. (A)** *UAS-TransTango/+* control, showing
1335 background GFP expression in mushroom bodies and Tomato+ signal in sub-aesophageal ganglion (SOG).
1336 **(B)** *DNT-2GAL4>UAS-TransTango*, revealing the GFP+ DNT-2 neurons and Tomato+ signal in DNT-2 neurons.
1337 TransTango also reveals what appears to be feedback connections between DNT-2 neurons from SMP to
1338 PRW (arrow). These are controls for Figure 2A. Scale bars: (A,B) 50µm. For further genotypes and sample
1339 sizes, see Supplementary Table S2.

1340

1341 **Supplementary Figure S4 Neuronal activity increased production and cleavage of DNT-2. (A)**
1342 Thermogenetic activation of DNT-2 neurons increased the number of DNT-2FLGFP+ vesicles or spots (*DNT-*
1343 *2>DNT-2-FL-GFP*, *TrpA1* with anti-GFP). Control 18°C: Unpaired Student t test, ns. Activation 30°C 24h:

1344 Mann Whitney**. (B)** Western blot from fly heads over-expressing DNT-2FL-GFP in DNT-2 neurons showing
1345 that neuronal activation with TrpA1 at 30°C increased DNT-2FL-GFP cleavage. **(**Genotype: *DNT-2>TrpA1,*
1346 *DNT-2FL-GFP*). Controls are flies of the same genotype kept constantly at 18°C as well as flies treated also
1347 at 30°C but lacking TrpA1. High temperature (30°C) is sufficient to increase fly activity. ***p<0.001. ns= not
1348 significant. For further genotypes, sample sizes, p values and other statistical details see Supplementary
1349 Table S2.
1350
1351 **Supplementary Figure S5** **Controls for Figure 5B.** Control at 18°C, for Figure 5B. DNT-2 bidirectional
1352 arborisation at SMP was visualised with Homer-GCaMP and anti-GFP antibodies (*DNT-21>homer-GCAMP*
1353 and *DNT-2>homer-GCAMP, TrpA1* at 18°C). Unpaired Student t-test, ns. Scale bars: (A,B) 30µm. For further
1354 genotypes, sample sizes, p values and other statistical details see Supplementary Table S2.
1355
1356 **Supplementary Figure S6** **Locomotion in open arena controls. (A)** Controls for Figure 6E. In 18°C
1357 controls, GAL80 is on and GAL4 is off, thus there is no adult specific *DNT-2FL* overexpression in DNT-2
1358 neurons in these flies. (Genotype: *tubGAL80ts, DNT-2>DNT-2FL*). Consistently, there was no increase in
1359 locomotion speed in an open arena, in flies over-expressing *DNT-2FL* relative to controls, compare also to
1360 Figure 6E. Kruskal Wallis ANOVA ns (lower median in *UAS-DNT-2FL/+* control). **(B)** Controls for Figure 6F.
1361 The cation TrpA1 opens at high temperatures (e.g. 30°C) but remains closed at 18°C. Consistently, there
1362 was no effect in locomotion at 18°C in flies of genotype *DNT-2>TrpA1* compared to controls, compare also
1363 to 30°C data in Figure 6F. Kruskal Wallis ANOVA ns. For further genotypes, sample sizes, p values and other
1364 statistical details see Supplementary Table S2.
1365
1366 **Supplementary Figure S7** **Altering *DNT-2* levels induced seizures.** Knock-down or over-expression of
1367 *DNT-2* in the adult, using $GAL80^{ts}$. Fruit-flies were reared at 18°C from egg laying to adult eclosion, when
1368 they were transferred to 30°C and kept there for 5 days prior to testing**.** To test for seizures, we used the
1369 bang-sensitivity test. $DNT2^{37}/DNT2^{18}$ mutant flies (left) and adult *DNT-2* knock-down flies ($tubGal80^{ts}$ *DNT-*

1370 *2Gal4>DNT-2RNAi,* centre) took longer to recover than controls. Over-expression of *DNT-2FL* in DNT-2

1371 neurons (*tubGal80^{ts} DNT-2Gal4>DNT-2FL,* right) increased variability in recovery time. For further

1372 genotypes and sample sizes see Supplementary Table S2.

1373

1374 **Table S1 Expression of *Tolls, keks* and Toll downstream adaptors in cells related to DNT-2A**

1375 **neurons.** Genes expressed in DNT-2 neurons, their potential and/or experimentally verified inputs and

1376 outputs, were identified with a combination of reporters (this work) and data from public single-cell

1377 RNAseq databases.

1378

1379 **Table S2 Statistical analysis.** Table providing full genotypes, sample sizes, statistical tests, multiple

1380 comparison corrections and p values.

1381

1382

FIGURE 1 Neurons expressing *DNT-2* and its receptors *Toll-6* and *kek-6* in the adult brain

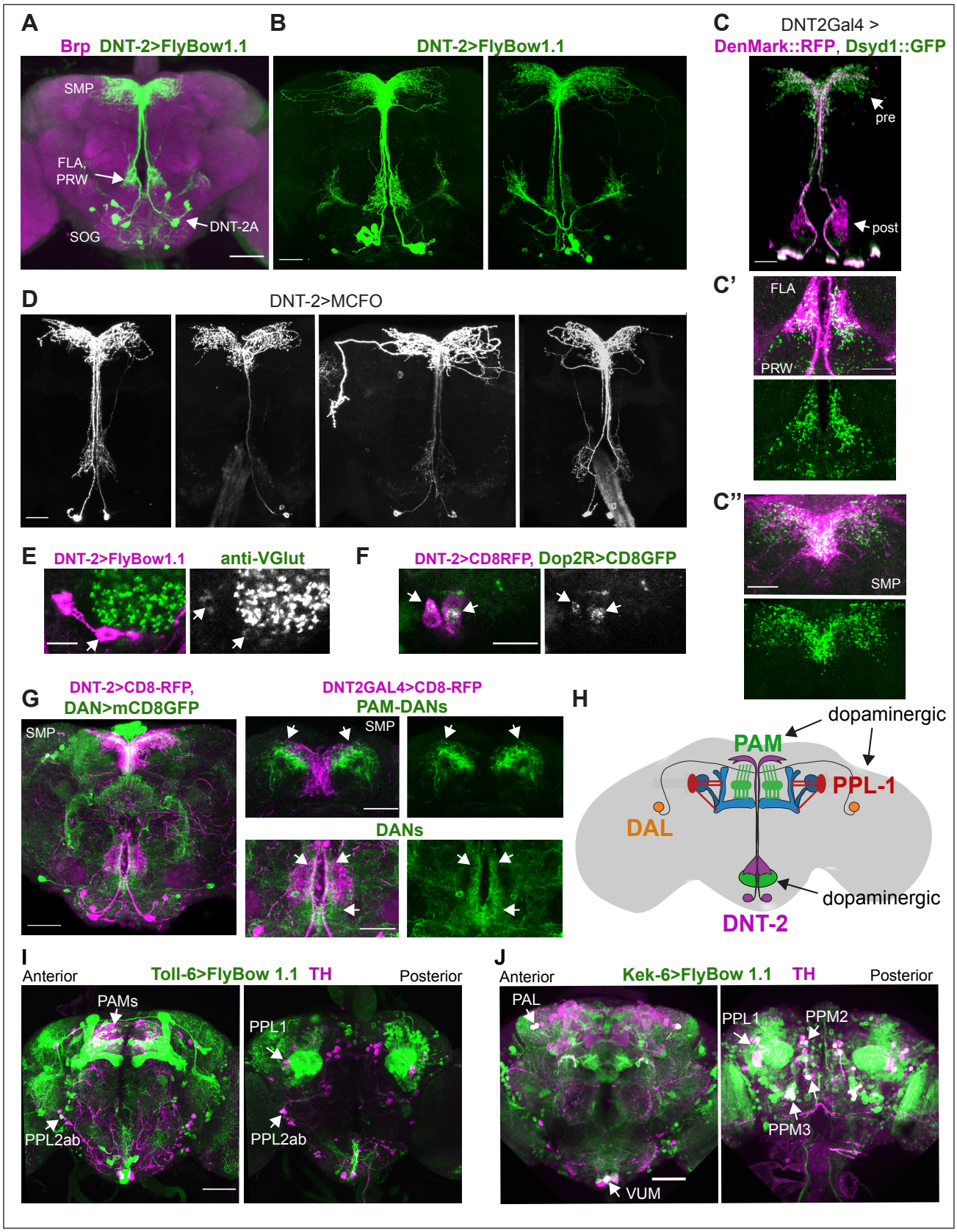

Figure 2 DNT-2 neurons are functionally connected to dopaminergic neurons

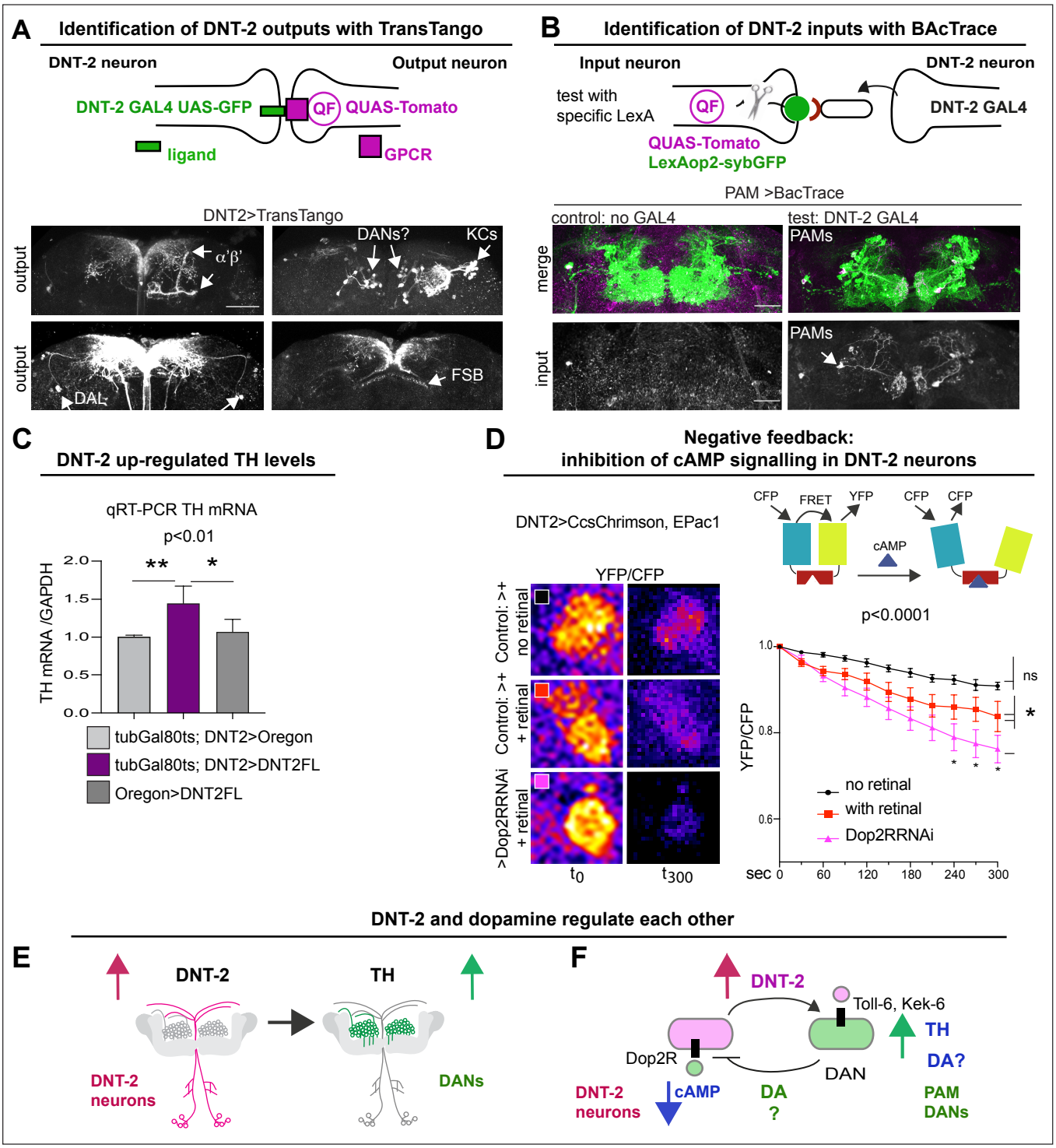

Figure 3 DNT-2 and Toll-6 maintain PAM neuron survival in the developing and adult brain

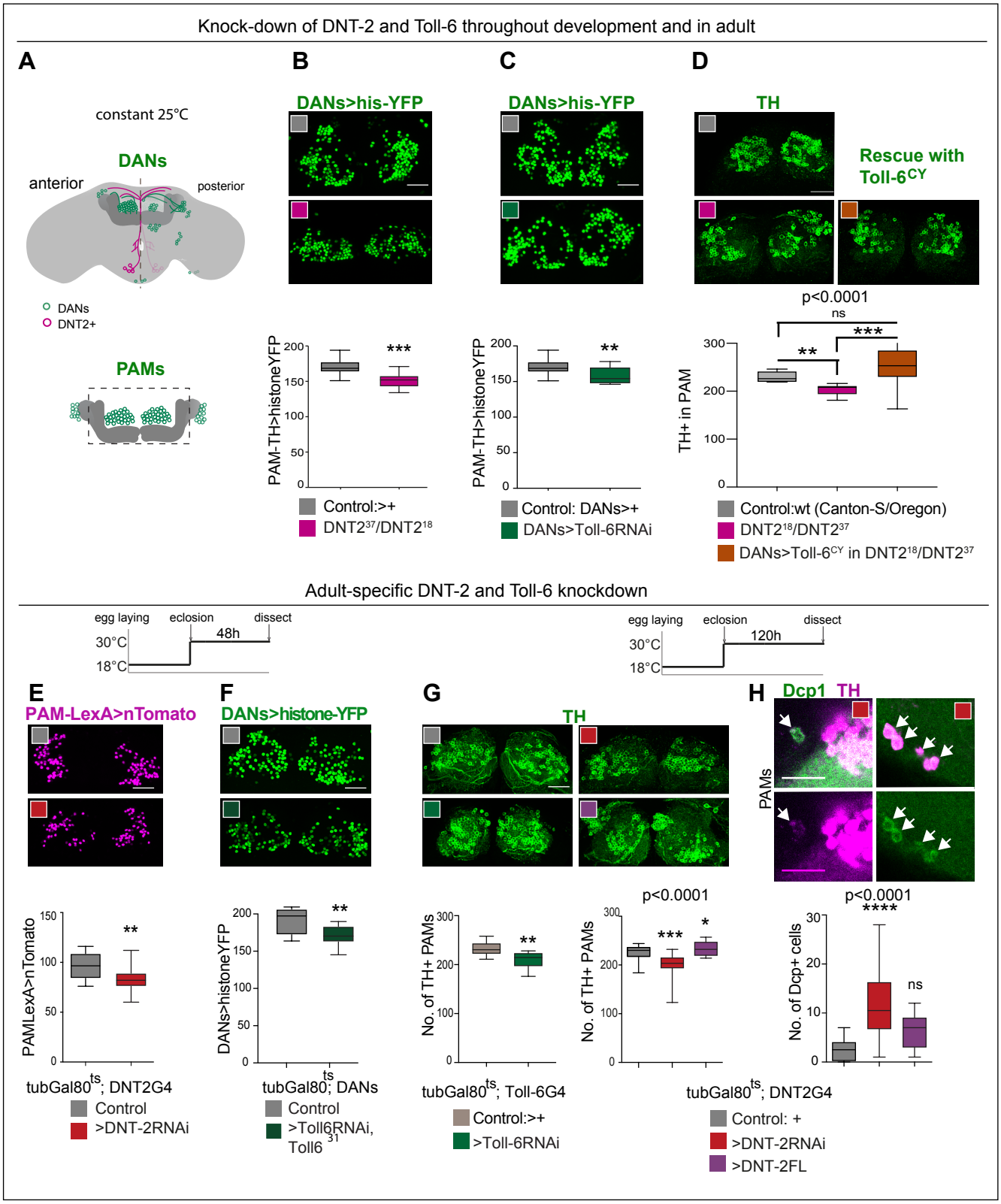

Figure 4 DNT-2, Toll-6 and Kek-6 are required for synapse formation and arborisations

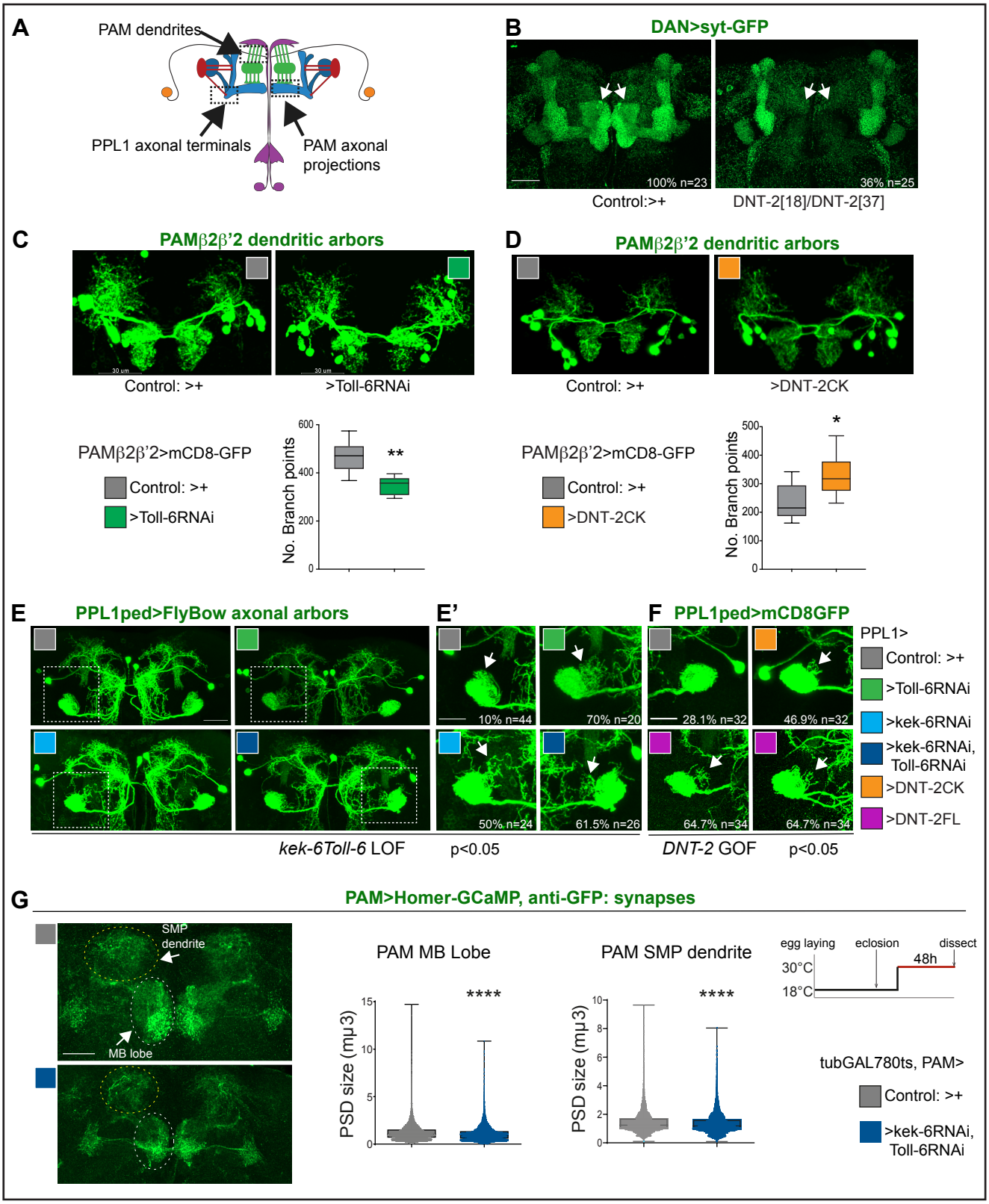

Figure 5 DNT-2 neuron activation and DNT-2 over-expression induce synaptogenesis

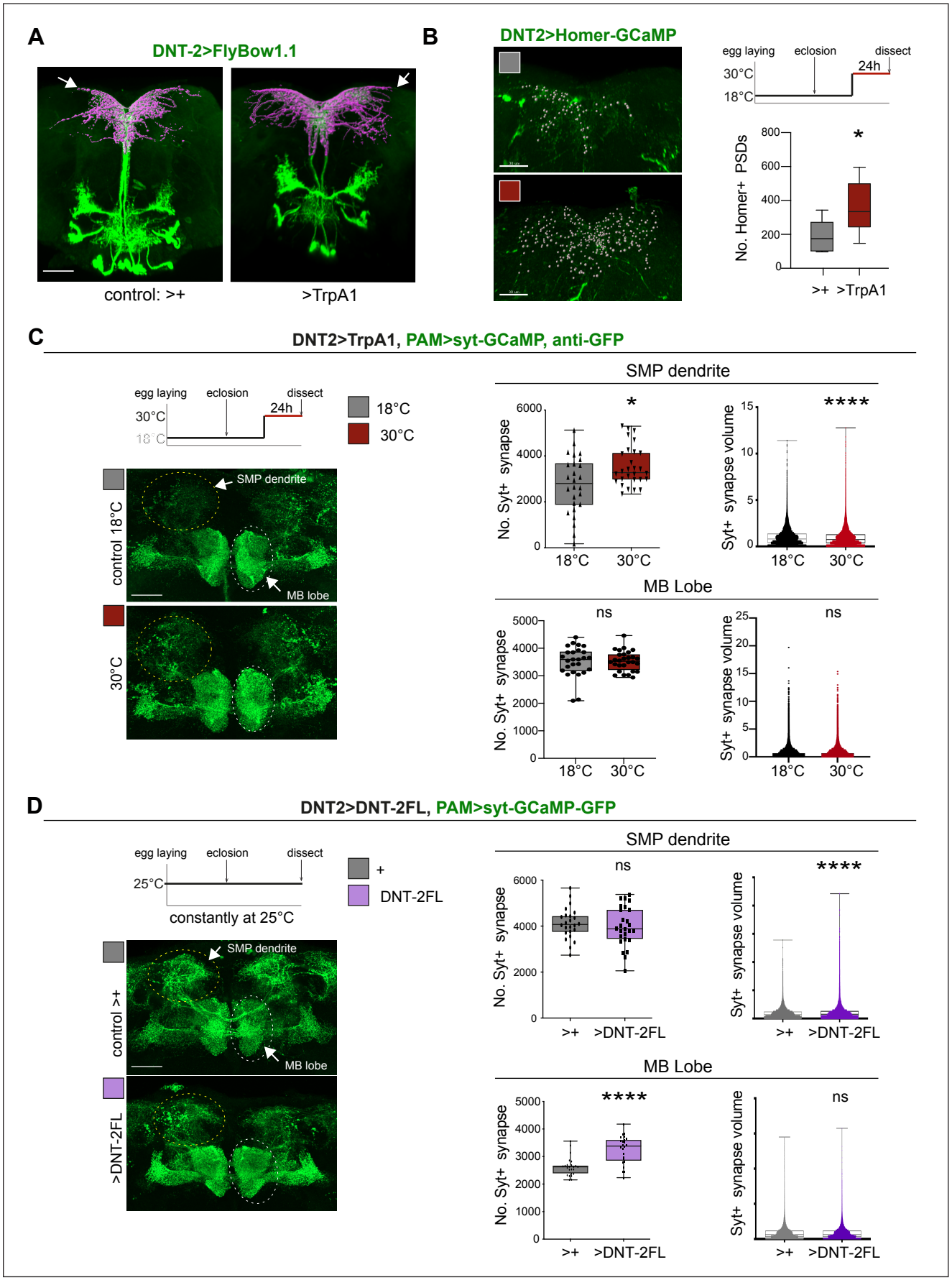
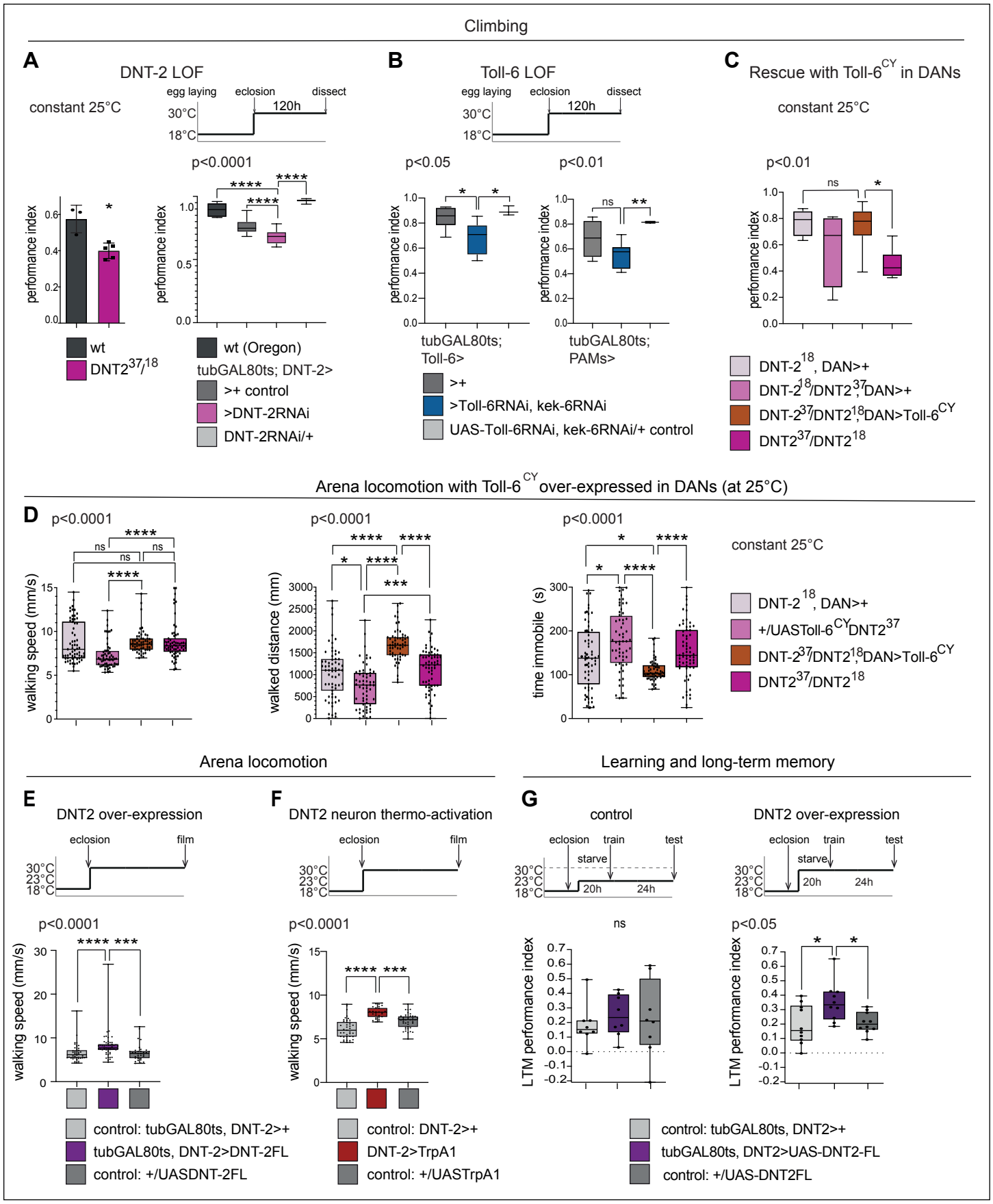
Figure 6 DNT-2-induced circuit plasticity modified dopamine-dependent behaviours.